Chapter 15

The Planar Laplace Equation

The fundamental partial differential equations that govern the equilibrium mechanics of multi-dimensional media are the Laplace equation and its inhomogeneous counterpart, the Poisson equation. The Laplace equation is arguably the most important differential equation in all of applied mathematics. It arises in an astonishing variety of mathematical and physical systems, ranging through fluid mechanics, electromagnetism, potential theory, solid mechanics, heat conduction, geometry, probability, number theory, and on and on. The solutions to the Laplace equation are known as "harmonic functions", and the discovery of their many remarkable properties forms one of the most significant chapters in the history of mathematics.

In this chapter, we concentrate on the Laplace and Poisson equations in a two-dimensional (planar) domain. Their status as equilibrium equations implies that the solutions are determined by their values on the boundary of the domain. As in the one-dimensional equilibrium boundary value problems, the principal cases are Dirichlet or fixed, Neumann or free, and mixed boundary conditions arise. In the introductory section, we shall briefly survey the basic boundary value problems associated with the Laplace and Poisson equations. We also take the opportunity to summarize the crucially important tripartite classification of planar second order partial differential equations: *elliptic*, such as the Laplace equation; *parabolic*, such as the heat equation; and *hyperbolic*, such as the wave equation. Each species has quite distinct properties, both analytical and numerical, and each forms an essentially distinct discipline. Thus, by the conclusion of this chapter, you will have encountered all three of the most important genres of partial differential equations.

The most important general purpose method for constructing explicit solutions of linear partial differential equations is the method of separation of variables. The method will be applied to the Laplace and Poisson equations in the two most important coordinate systems — rectangular and polar. Linearity implies that we may combine the separable solutions, and the resulting infinite series expressions will play a similar role as for the heat and wave equations. In the polar coordinate case, we can, in fact, sum the infinite series in closed form, leading to the explicit Poisson integral formula for the solution. More sophisticated techniques, relying on complex analysis, but (unfortunately) only applicable to the two-dimensional case, will be deferred until Chapter 16.

Green's formula allows us to properly formulate the Laplace and Poisson equations in self-adjoint, positive definite form, and thereby characterize the solutions via a minimization principle, first proposed by the nineteenth century mathematician Lejeune Dirichlet, who also played a crucial role in putting Fourier analysis on a rigorous foundation. Minimization forms the basis of the most important numerical solution technique — the finite

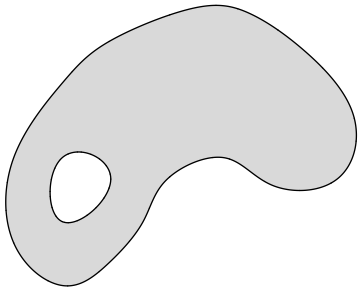

Figure 15.1. Planar Domain.

element method that we first encountered in Chapter 11. In the final section, we discuss numerical solution techniques based on finite element analysis for the Laplace and Poisson equations and their elliptic cousins, including the Helmholtz equation and more general positive definite boundary value problems.

15.1. The Planar Laplace Equation.

The two-dimensional *Laplace equation* is the second order linear partial differential equation

$$\frac{\partial^2 u}{\partial x^2} + \frac{\partial^2 u}{\partial y^2} = 0. \tag{15.1}$$

It is named in honor of the outstanding eighteenth century French mathematician Pierre–Simon Laplace. Along with the heat and wave equations, it completes the trinity of truly fundamental partial differential equations. A real-valued solution $u(x, y)$ to the Laplace equation is known as a *harmonic function*. The space of harmonic functions can thus be identified as the kernel of the second order linear partial differential operator

$$\Delta = \frac{\partial^2}{\partial x^2} + \frac{\partial^2}{\partial y^2}\,, \tag{15.2}$$

known as the *Laplace operator*, or *Laplacian* for short. The inhomogeneous or forced version, namely

$$-\Delta[u] = -\frac{\partial^2 u}{\partial x^2} - \frac{\partial^2 u}{\partial y^2} = f(x, y) \tag{15.3}$$

is known as *Poisson's equation*, named for Siméon–Denis Poisson, who was taught by Laplace. Poisson's equation can be viewed as the higher dimensional analogue of the basic equilibrium equation (11.12) for a bar.

The Laplace and Poisson equations arise as the basic equilibrium equations in a remarkable variety of physical systems. For example, we may interpret $u(x, y)$ as the displacement of a *membrane*, e.g., a drum skin; the inhomogeneity $f(x, y)$ in the Poisson equation represents an external forcing. Another example is in the thermal equilibrium of flat plates; here $u(x, y)$ represents the temperature and $f(x, y)$ an external heat source. In fluid mechanics, $u(x, y)$ represents the potential function whose gradient $\mathbf{v} = \nabla u$ is the velocity vector of a steady planar fluid flow. Similar considerations apply to two-dimensional electrostatic and gravitational potentials. The dynamical counterparts to the

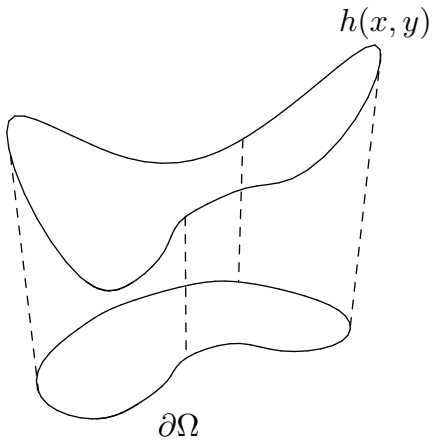

Figure 15.2. Dirichlet Boundary Conditions.

Laplace equation are the higher dimensional versions of the heat and wave equations, to be analyzed in Chapter 17.

Since both the Laplace and Poisson equations describe equilibrium configurations, they arise in applications in the context of boundary value problems. We seek a solution $u(x,y)$ to the partial differential equation defined on a fixed bounded, open domain[†] $(x,y) \in \Omega \subset \mathbb{R}^2$. The solution is required to satisfy suitable conditions on the boundary of the domain, denoted $\partial\Omega$, which will consist of one or more simple, closed curves, as illustrated in Figure 15.1. As in one-dimensional equilibria, there are three especially important types of boundary conditions.

The first are the *fixed* or *Dirichlet boundary conditions*, which specify the value of the function u on the boundary:

$$u(x,y) = h(x,y) \qquad \text{for} \qquad (x,y) \in \partial\Omega. \tag{15.4}$$

The Dirichlet conditions (15.4) serve to uniquely specify the solution $u(x,y)$ to the Laplace or the Poisson equation. Physically, in the case of a free or forced membrane, the Dirichlet boundary conditions correspond to gluing the edge of the membrane to a wire at height $h(x,y)$ over each boundary point $(x,y) \in \partial\Omega$, as illustrated in Figure 15.2. Uniqueness means that the shape of the boundary wire will unambiguously specify the vertical displacement of the membrane in equilibrium. Similarly, in the modeling of thermal equilibrium, a Dirichlet boundary condition represents the imposition of a prescribed temperature distribution, represented by the function h, along the boundary of the plate.

The second important class are the *Neumann boundary conditions*

$$\frac{\partial u}{\partial \mathbf{n}} = \nabla u \cdot \mathbf{n} = k(x,y) \qquad \text{on} \qquad \partial\Omega, \tag{15.5}$$

in which the normal derivative of the solution u on the boundary is prescribed. For example, in thermomechanics, a Neumann boundary condition specifies the heat flux into the

[†] See Appendix A for the precise definitions of the terms "domain", "bounded", "boundary", etc.

plate through its boundary. The "no-flux" or homogeneous Neumann boundary conditions, where $k(x, y) \equiv 0$, correspond to a fully insulated boundary. In the case of a membrane, homogeneous Neumann boundary conditions correspond to an unattached edge of the drum. In fluid mechanics, the no-flux conditions imply that the normal component of the velocity vector $\mathbf{v} = \nabla u$ vanishes on the boundary, and so no fluid is allowed to flow across the solid boundary.

Finally, one can mix the previous two sorts of boundary conditions, imposing Dirichlet conditions on part of the boundary, and Neumann on the complementary part. The general *mixed boundary value problem* has the form

$$-\Delta u = f \quad \text{in} \quad \Omega, \qquad u = h \quad \text{on} \quad D, \qquad \frac{\partial u}{\partial \mathbf{n}} = k \quad \text{on} \quad N, \tag{15.6}$$

with the boundary $\partial\Omega = D \cup N$ being the disjoint union of a "Dirichlet part", denoted by D, and a "Neumann part" N. For example, if u represents the equilibrium temperature in a plate, then the Dirichlet part of the boundary is where the temperature is fixed, while the Neumann part is insulated, or, more generally, has prescribed heat flux. Similarly, when modeling the displacement of a membrane, the Dirichlet part is where the edge of the drum is attached to a support, while the homogeneous Neumann part is where it is left hanging free.

Classification of Linear Partial Differential Equations in Two Variables

We have, at last, encountered all three of the fundamental linear, second order, partial differential equations for functions of two variables. The homogeneous versions of the trinity are

(*a*)	The wave equation:	$u_{tt} - c^2\, u_{xx} = 0,$	*hyperbolic*,
(*b*)	The heat equation:	$u_t - \gamma\, u_{xx} = 0,$	*parabolic*,
(*c*)	Laplace's equation:	$u_{xx} + u_{yy} = 0,$	*elliptic.*

The last column specifies the equations' *type*, in accordance with the standard taxonomy of partial differential equations. An explanation of the terminology will appear momentarily.

The wave, heat and Laplace equations are the prototypical representatives of the three fundamental genres of partial differential equations, each with its own intrinsic features and physical manifestations. Equations governing vibrations, such as the wave equation, are typically hyperbolic. Equations governing diffusion, such as the heat equation, are parabolic. Hyperbolic and parabolic equations both govern dynamical processes, and one of the variables is identified with the time. On the other hand, equations modeling equilibrium phenomena, including the Laplace and Poisson equations, are typically elliptic, and only involve spatial variables. Elliptic partial differential equations are associated with boundary value problems, whereas parabolic and hyperbolic equations require initial-boundary value problems, with, respectively, one or two required initial conditions. Furthermore, each type requires a fundamentally different kind of numerical solution algorithm.

While the initial tripartite classification first appears in partial differential equations in two variables, the terminology, underlying properties, and assocaited physical models

carry over to equations in higher dimensions. Most of the important partial differential equations arising in applications are of one of these three types, and it is fair to say that the field of partial differential equations breaks into three major, disjoint subfields. Or, rather four subfields, the last being all the equations, including higher order equations, that do not fit into this preliminary categorization.

The classification of linear, second order partial differential equations for a scalar-valued function $u(x, y)$ of two variables[†] proceeds as follows. The most general such equation has the form

$$L[u] = A\,u_{xx} + 2\,B\,u_{xy} + C\,u_{yy} + D\,u_x + E\,u_y + F\,u = f, \tag{15.7}$$

where the coefficients A, B, C, D, E, F are all allowed to be functions of (x, y), as is the inhomogeneity or forcing function $f = f(x, y)$. The equation is *homogeneous* if and only if $f \equiv 0$. We assume that at least one of the leading coefficients A, B, C is nonzero, as otherwise the equation degenerates to a first order equation.

The key quantity that determines the *type* of such a partial differential equation is its *discriminant*

$$\Delta = B^2 - AC. \tag{15.8}$$

This should (and for good reason) remind the reader of the discriminant of the quadratic equation

$$Q(\xi, \eta) = A\,\xi^2 + 2\,B\,\xi\,\eta + C\,\eta^2 + D\,\xi + E\,\eta + F = 0. \tag{15.9}$$

The solutions (ξ, η) describes a plane curve — namely, a conic section. In the nondegenerate cases, the discriminant determines its geometrical type; it is

- a hyperbola when $\Delta > 0$,
- a parabola when $\Delta = 0$, or
- an ellipse when $\Delta < 0$.

This tripartite classification provides the underlying motivation for the terminology used to classify second order partial differential equations.

Definition 15.1. At a point (x, y), the linear, second order partial differential equation (15.7) is called

(a) hyperbolic		$\Delta(x, y) > 0$,
(b) parabolic	if and only if	$\Delta(x, y) = 0$, but $A^2 + B^2 + C^2 \neq 0$,
(c) elliptic		$\Delta(x, y) < 0$,
(d) degenerate		$A = B = C = 0$.

In particular:

- The wave equation $u_{xx} - u_{yy} = 0$ has discriminant $\Delta = 1$, and is hyperbolic.
- The heat equation $u_{xx} - u_y = 0$ has discriminant $\Delta = 0$, and is parabolic.
- The Poisson equation $u_{xx} + u_{yy} = -f$ has discriminant $\Delta = -1$, and is elliptic.

[†] For dynamical equations, we will identify y as the time variable t.

Example 15.2. Since the coefficients in the partial differential equation are allowed to vary over the domain, the type of an equation may vary from point to point. Equations that change type are much less common, as well as being much harder to handle. One example arising in the theory of supersonic aerodynamics is the *Tricomi equation*

$$y\,u_{xx} - u_{yy} = 0. \tag{15.10}$$

Comparing with (15.7), we find that

$$A = y, \qquad C = -1, \qquad \text{and} \qquad B = D = E = F = f = 0.$$

The discriminant in this particular case is $\Delta = y$, and hence the equation is hyperbolic when $y > 0$, elliptic when $y < 0$, and parabolic on the transition line $y = 0$. The hyperbolic region corresponds to subsonic fluid flow, while the supersonic regions are of elliptic type. The transitional parabolic boundary represents the shock line between the sub- and supersonic regions.

Characteristics

In Section 14.5, we learned the importance of the characteristic lines in understanding the behavior of solutions to the wave equation. Characteristic curves play a similarly fundamental role in the study of more general linear hyperbolic partial differential equations. Indeed, characteristics are another means of distinguishing between the three classes of second order partial differential equations.

Definition 15.3. A smooth curve $\mathbf{x}(t) \subset \mathbb{R}^2$ is called a *characteristic curve* for the second order partial differential equation (15.7) if its tangent vector $\dot{\mathbf{x}} = (\dot{x}, \dot{y})^T$ satisfies the quadratic *characteristic equation*

$$A(x,y)\,\dot{y}^2 - 2\,B(x,y)\,\dot{x}\,\dot{y} + C(x,y)\,\dot{x}^2 = 0. \tag{15.11}$$

Pay careful attention to the form of the characteristic equation — the positions of $\dot{x}$ and $\dot{y}$ are the opposite of what you might expect, while a minus sign appears in front of B. Furthermore, only the highest order terms in the original partial differential equation play a role; the first and zero$^{\text{th}}$ order terms are irrelevant as far as its characteristics go.

For example, consider the hyperbolic wave equation[†]

$$-c^2\,u_{xx} + u_{yy} = 0.$$

In this case, $A = -c^2$, $B = 0$, $C = 1$, and so (15.11) takes the form

$$-c^2\,\dot{y}^2 + \dot{x}^2 = 0, \qquad \text{which implies that} \qquad \dot{x} = \pm\, c\,\dot{y}.$$

All solutions to the latter ordinary differential equations are straight lines

$$x = \pm\, c\,y + k, \tag{15.12}$$

[†] *Warning*: Here, we regard y as the "time" variable in the differential equation, rather than t, which assumes the role of the curve parameter.

where k is an integration constant. Therefore, the wave equation has two characteristic curves passing through each point (a, b), namely the straight lines (15.12) of slope $\pm c$, in accordance with our earlier definition of characteristics. In general, a linear partial differential equation is hyperbolic at a point (x, y) if and only if there are two characteristic curves passing through it. Moreover, as with the wave equation, disturbances that are concentrated near the point will tend to propagate along the characteristic curves. This fact lies at the foundation of geometric optics. Light rays move along characteristic curves, and are thereby subject to the optical phenomena of refraction and focusing.

On the other hand, the elliptic Laplace equation

$$u_{xx} + u_{yy} = 0$$

has no (real) characteristic curves since the characteristic equation (15.11) reduces to

$$\dot{y}^2 + \dot{x}^2 = 0.$$

Elliptic equations have no characteristics, and as a consequence, do not admit propagating signals; the effect of a localized disturbance, say on a membrane, is immediately felt everywhere.

Finally, for the parabolic heat equation

$$u_{xx} - u_y = 0,$$

the characteristic equation is simply

$$\dot{y}^2 = 0,$$

and so there is only one characteristic curve through each point (a, b), namely the horizontal line $y = b$. Indeed, our observation that the effect of an initial concentrated heat source is immediately felt all along the bar is in accordance with propagation of localized disturbances along the characteristics.

In this manner, elliptic, parabolic, and hyperbolic partial differential equations are distinguished by the number of (real) characteristic curves passing through a point — namely, zero, one and two, respectively. Further discussion of characteristics and their applications to solving both linear and nonlinear partial differential equations can be found in Section 22.1.

15.2. Separation of Variables.

One of the oldest — and still one of the most widely used — techniques for constructing explicit analytical solutions to partial differential equations is the method of *separation of variables*. We have, in fact, already used separation of variables to construct particular solutions to the heat and wave equations. In each case, we sought a solution in the form of a product, $u(t, x) = h(t)\, v(x)$, of scalar functions of each individual variable. For the heat and similar parabolic equations, $h(t)$ was an exponential, while the wave equation chose a trigonometric function. In more general situations, we might not know in advance which function $h(t)$ is appropriate. When the method succeeds (which is not guaranteed in advance), both factors are found as solutions to certain ordinary differential equations.

Turning to the Laplace equation, the solution depends on x and y, and so the multiplicative separation of variables ansatz has the form

$$u(x,y) = v(x)\, w(y). \tag{15.13}$$

Let us see whether such a function can solve the Laplace equation by direct substitution. First of all,

$$\frac{\partial^2 u}{\partial x^2} = v''(x)\, w(y), \qquad \frac{\partial^2 u}{\partial y^2} = v(x)\, w''(y),$$

where the primes indicate ordinary derivatives, and so

$$\Delta u = \frac{\partial^2 u}{\partial x^2} + \frac{\partial^2 u}{\partial y^2} = v''(x)\, w(y) + v(x)\, w''(y) = 0.$$

The method will succeed if we are able to separate the variables by placing all of the terms involving x on one side of the equation and all the terms involving y on the other. Here, we first write the preceding equation in the form

$$v''(x)\, w(y) = -\, v(x)\, w''(y).$$

Dividing both sides by $v(x)\, w(y)$ (which we assume is not identically zero as otherwise the solution would be trivial) yields

$$\frac{v''(x)}{v(x)} = -\,\frac{w''(y)}{w(y)}\,, \tag{15.14}$$

which effectively "separates" the x and y variables on each side of the equation. Now, how could a function of x alone be equal to a function of y alone? A moment's reflection should convince the reader that this can happen if and only if the two functions are constant[†], so

$$\frac{v''(x)}{v(x)} = -\,\frac{w''(y)}{w(y)} = \lambda,$$

where we use λ to indicate the common *separation constant*. Thus, the individual factors $v(x)$ and $w(y)$ satisfy ordinary differential equations

$$v'' - \lambda\, v = 0, \qquad w'' + \lambda\, w = 0,$$

as promised.

We already know how to solve both of these ordinary differential equations by elementary techniques. There are three different cases, depending on the sign of the separation constant λ, each leading to four different solutions to the Laplace equation. We collect the entire family of separable harmonic functions together in the following table.

[†] Technical detail: one should assume that the underlying domain be connected for this to be valid; however, in practical analysis, this technicality is irrelevant.

λ	$v(x)$	$w(y)$	$u(x,y) = v(x)\,w(y)$
$\lambda = -\omega^2 < 0$	$\cos \omega x,\ \sin \omega x$	$e^{-\omega y},\ e^{\omega y},$	$e^{\omega y}\cos \omega x,\quad e^{\omega y}\sin \omega x,$ $e^{-\omega y}\cos \omega x,\quad e^{-\omega y}\sin \omega x$
$\lambda = 0$	$1,\ x$	$1,\ y$	$1,\ x,\ y,\ x\,y$
$\lambda = \omega^2 > 0$	$e^{-\omega x},\ e^{\omega x}$	$\cos \omega y,\ \sin \omega y$	$e^{\omega x}\cos \omega y,\quad e^{\omega x}\sin \omega y,$ $e^{-\omega x}\cos \omega y,\quad e^{-\omega x}\sin \omega y$

Since Laplace's equation is a homogeneous linear system, any linear combination of solutions is also a solution. Thus, we can try to build general solutions as finite linear combinations, or, provided we pay proper attention to convergence issues, infinite series in the separable solutions. To solve boundary value problems, one must ensure that the resulting combination satisfies the boundary conditions. This is not easy, unless the underlying domain has a rather specific geometry.

In fact, the only domains for which we can explicitly solve boundary value problems using the separable solutions constructed above are rectangles. In this manner, we are led to consider boundary value problems for Laplace's equation

$$\Delta u = 0 \qquad \text{on a rectangle} \qquad R = \{\, 0 < x < a,\ \ 0 < y < b \,\}. \tag{15.15}$$

To be completely specific, we will focus on the following Dirichlet boundary conditions:

$$u(x,0) = f(x), \qquad u(x,b) = 0, \qquad u(0,y) = 0, \qquad u(a,y) = 0. \tag{15.16}$$

It will be important to only allow a nonzero boundary condition on one of the four sides of the rectangle. Once we know how to solve this type of problem, we can employ linear superposition to solve the general Dirichlet boundary value problem on a rectangle; see Exercise ■ for details. Other boundary conditions can be treated in a similar fashion — with the proviso that the condition on each side of the rectangle is either entirely Dirichlet or entirely Neumann.

We will ensure that the series solution we construct satisfies the three homogeneous boundary conditions by only using separable solutions that satisfy them. The remaining nonzero boundary condition will then specify the coefficients of the individual summands. The function $u(x,y) = v(x)\,w(y)$ will vanish on the top, right and left sides of the rectangle provided

$$v(0) = v(a) = 0, \qquad \text{and} \qquad w(b) = 0.$$

Referring to the preceding table, the first condition $v(0) = 0$ requires

$$v(x) = \begin{cases} \sin \omega x, & \lambda = \omega^2 > 0, \\ x, & \lambda = 0, \\ \sinh \omega x, & \lambda = -\omega^2 < 0, \end{cases}$$

where $\sinh z = \frac{1}{2}(e^z - e^{-z})$ is the usual hyperbolic sine function. However, the second and third cases cannot satisfy the second boundary condition $v(a) = 0$, and so we discard them. The first case leads to the condition

$$v(a) = \sin \omega\, a = 0, \qquad \text{and hence} \qquad \omega\, a = \pi, 2\pi, 3\pi, \dots$$

is an integral multiple of π. Therefore, the separation constant

$$\lambda = \omega^2 = \frac{n^2 \pi^2}{a^2}, \qquad \text{where} \qquad n = 1, 2, 3, \dots, \tag{15.17}$$

and the corresponding functions are

$$v(x) = \sin \frac{n \pi x}{a}, \qquad n = 1, 2, 3, \dots. \tag{15.18}$$

Note: We have merely recomputed the known eigenvalues and eigenfunctions of the familiar boundary value problem $v'' + \lambda\, v = 0$, $v(0) = v(a) = 0$.

Since $\lambda = \omega^2 > 0$, the third boundary condition $w(b) = 0$ requires that, up to constant multiple,

$$w(y) = \sinh \omega\,(b - y) = \sinh \frac{n \pi\,(b - y)}{a}. \tag{15.19}$$

Therefore, each of the separable solutions

$$u_n(x, y) = \sin \frac{n \pi x}{a}\ \sinh \frac{n \pi\,(b - y)}{a}, \qquad n = 1, 2, 3, \dots, \tag{15.20}$$

satisfies the three homogeneous boundary conditions. It remains to analyze the inhomogeneous boundary condition along the bottom edge of the rectangle. To this end, let us try a linear superposition of the separable solutions in the form of an infinite series

$$u(x, y) = \sum_{n=1}^{\infty} c_n\, u_n(x, y) = \sum_{n=1}^{\infty} c_n\, \sin \frac{n \pi x}{a}\ \sinh \frac{n \pi\,(b - y)}{a},$$

whose coefficients $c_1, c_2, \dots$ are to be prescribed by the remaining boundary condition. At the bottom edge, $y = 0$, we find

$$u(x, 0) = \sum_{n=1}^{\infty} c_n\, \sinh \frac{n \pi\, b}{a}\ \sin \frac{n \pi x}{a} = f(x), \qquad 0 \le x \le a, \tag{15.21}$$

which takes the form of a Fourier sine series for the function $f(x)$. According to (12.84), the coefficients b_n of the Fourier sine series

$$f(x) = \sum_{n=1}^{\infty} b_n\, \sin \frac{n \pi x}{a} \qquad \text{are given by} \qquad b_n = \frac{2}{a} \int_0^a f(x) \sin \frac{n \pi x}{a}\, dx. \tag{15.22}$$

Comparing (15.21, 22), we discover that

$$c_n \sinh \frac{n \pi b}{a} = b_n \qquad \text{or} \qquad c_n = \frac{b_n}{\sinh \dfrac{n \pi\, b}{a}} = \frac{2}{a \sinh \dfrac{n \pi\, b}{a}} \int_0^a f(x) \sin \frac{n \pi x}{a}\, dx.$$

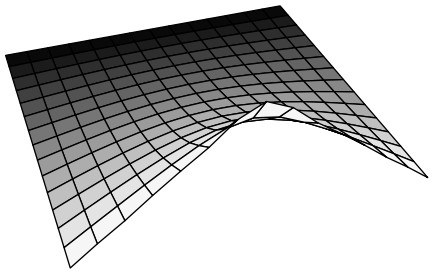

Figure 15.3. Square Membrane on a Wire.

Therefore, the solution to the boundary value problem takes the form of an infinite series

$$u(x,y) = \sum_{n=1}^{\infty} b_n \sin \frac{n\pi x}{a} \, \frac{\sinh \dfrac{n\pi (b-y)}{a}}{\sinh \dfrac{n\pi b}{a}}, \tag{15.23}$$

where b_n are the Fourier sine coefficients (15.22) of $f(x)$.

Does this series actually converge to the solution to the boundary value problem? Fourier analysis says that, under very mild conditions on the boundary function $f(x)$, the answer is "yes". Suppose that its Fourier coefficients are uniformly bounded,

$$| b_n | \leq M \qquad \text{for all} \qquad n \geq 1, \tag{15.24}$$

which, according to (14.23) is true whenever $f(x)$ is piecewise continuous or, more generally, integrable: $\displaystyle\int_0^a | f(x) | \, dx < \infty$. Boundedness is also satisfied by many generalized functions, such as the delta function. In this case, as you are asked to prove in Exercise ■, the coefficients of the Fourier sine series (15.23)

$$B_n \;=\; \frac{\sinh \dfrac{n\pi (b-y)}{a}}{\sinh \dfrac{n\pi b}{a}} \, b_n \quad \longrightarrow \quad 0 \qquad \text{as} \qquad n \longrightarrow \infty \tag{15.25}$$

exponentially fast for all $0 < y \leq b$. Thus, according to Section 12.3, the solution $u(x,y)$ is an infinitely differentiable function of x at each point in the rectangle, and can be well approximated by partial summation. The solution is also infinitely differentiable with respect to y; see Exercise ■. In fact, as we shall see, the solutions to the Laplace equation are *always analytic* functions inside their domain of definition — even when their boundary values are rather rough.

Example 15.4. A membrane is stretched over a wire in the shape of a unit square

with one side bent in half, as graphed in Figure 15.3. The precise boundary conditions are

$$u(x,y) = \begin{cases} x, & 0 \le x \le \frac{1}{2}, & y = 0, \\ 1-x, & \frac{1}{2} \le x \le 1, & y = 0, \\ 0, & 0 \le x \le 1, & y = 1, \\ 0, & x = 0, & 0 \le y \le 1, \\ 0, & x = 1, & 0 \le y \le 1. \end{cases}$$

The Fourier sine series of the inhomogeneous boundary function is readily computed:

$$f(x) = \begin{cases} x, & 0 \le x \le \frac{1}{2}, \\ 1-x, & \frac{1}{2} \le x \le 1, \end{cases}$$
$$= \frac{4}{\pi^2}\left(\sin \pi x - \frac{\sin 3\pi x}{9} + \frac{\sin 5\pi x}{25} - \cdots\right) = \frac{4}{\pi^2}\sum_{m=0}^{\infty} (-1)^m \frac{\sin(2m+1)\pi x}{(2m+1)^2}.$$

Specializing (15.23) when $a = b = 1$, we conclude that the solution to the boundary value problem is given by the Fourier series

$$u(x,y) = \frac{4}{\pi^2}\sum_{m=0}^{\infty} (-1)^m \frac{\sin(2m+1)\pi x \, \sinh(2m+1)\pi(1-y)}{(2m+1)^2 \sinh(2m+1)\pi}.$$

In Figure 15.3 we plot the sum of the first 10 terms in the series. This gives a reasonably good approximation to the actual solution, except when we are very close to the raised corner of the boundary wire — which is the point of maximal displacement of the membrane.

Polar Coordinates

The method of separation of variables can be successfully exploited in certain other very special geometries. One particularly important case is a circular disk. To be specific, let us take the disk to have radius 1 and centered at the origin. Consider the Dirichlet boundary value problem

$$\Delta u = 0, \qquad x^2 + y^2 < 1, \qquad \text{and} \qquad u = h, \qquad x^2 + y^2 = 1, \tag{15.26}$$

so that the function $u(x,y)$ satisfies the Laplace equation on the unit disk and satisfies the specified Dirichlet boundary conditions on the unit circle. For example, $u(x,y)$ might represent the displacement of a circular drum that is attached to a wire of height

$$h(x,y) = h(\cos\theta, \sin\theta) \equiv h(\theta), \qquad 0 \le \theta \le 2\pi, \tag{15.27}$$

above each point $(x,y) = (\cos\theta, \sin\theta)$ on the unit circle.

The rectangular separable solutions are not particularly helpful in this situation. The fact that we are dealing with a circular geometry inspires us to adopt polar coordinates

$$x = r\cos\theta, \qquad y = r\sin\theta, \qquad \text{or} \qquad r = \sqrt{x^2+y^2}, \qquad \theta = \tan^{-1}\frac{y}{x},$$

and write the solution $u(r,\theta)$ as a function thereof.

Warning: We will retain the same symbol, e.g., u, when rewriting a function in a different coordinate system. This is the convention of tensor analysis and differential geometry, [**2**], that treats the function or tensor as an intrinsic object, which is concretely realized through its formula in any chosen coordinate system. For instance, if $u(x,y) = x^2 + 2\,y$ in rectangular coordinates, then $u(r,\theta) = r^2\cos^2\theta + 2\,r\sin\theta$ — and *not* $r^2 + 2\,\theta$ — is its expression in polar coordinates. This convention avoids introducing new symbols when changing coordinates.

We also need to relate derivatives with respect to x and y to those with respect to r and θ. Performing a standard chain rule computation, we find

$$\begin{aligned} \frac{\partial}{\partial r} &= \cos\theta\,\frac{\partial}{\partial x} + \sin\theta\,\frac{\partial}{\partial y}\,, \\ \frac{\partial}{\partial \theta} &= -\,r\sin\theta\,\frac{\partial}{\partial x} + r\cos\theta\,\frac{\partial}{\partial y}\,, \end{aligned} \qquad \text{so} \qquad \begin{aligned} \frac{\partial}{\partial x} &= \cos\theta\,\frac{\partial}{\partial r} - \frac{\sin\theta}{r}\,\frac{\partial}{\partial \theta}\,, \\ \frac{\partial}{\partial y} &= \sin\theta\,\frac{\partial}{\partial r} + \frac{\cos\theta}{r}\,\frac{\partial}{\partial \theta}\,. \end{aligned} \tag{15.28}$$

These formulae allow us to rewrite the Laplace equation in polar coordinates; after some calculation in which many of the terms cancel, we find

$$\Delta u = \frac{\partial^2 u}{\partial x^2} + \frac{\partial^2 u}{\partial y^2} = \frac{\partial^2 u}{\partial r^2} + \frac{1}{r}\,\frac{\partial u}{\partial r} + \frac{1}{r^2}\,\frac{\partial^2 u}{\partial \theta^2} = 0. \tag{15.29}$$

The boundary conditions are imposed on the unit circle $r = 1$, and so, by (15.27), take the form

$$u(1,\theta) = h(\theta). \tag{15.30}$$

Keep in mind that, in order to be single-valued functions of x, y, the solution $u(r,\theta)$ and its boundary values $h(\theta)$ must both be $2\,\pi$ periodic functions of the angular coordinate:

$$u(r,\theta + 2\,\pi) = u(r,\theta), \qquad\qquad h(\theta + 2\,\pi) = h(\theta). \tag{15.31}$$

Polar separation of variables is based on the ansatz

$$u(r,\theta) = v(r)\,w(\theta) \tag{15.32}$$

that assumes that the solution is a product of functions of the individual polar variables. Substituting (15.32) into the polar form (15.29) of Laplace's equation, we find

$$v''(r)\,w(\theta) + \frac{1}{r}\,v'(r)\,w(\theta) + \frac{1}{r^2}\,v(r)\,w''(\theta) = 0.$$

We now separate variables by moving all the terms involving r onto one side of the equation and all the terms involving θ onto the other. This is accomplished by first multiplying the equation by $r^2/v(r)\,w(\theta)$, and then moving the last term to the right hand side:

$$\frac{r^2\,v''(r) + r\,v'(r)}{v(r)} = -\,\frac{w''(\theta)}{w(\theta)} = \lambda.$$

As in the rectangular case, a function of r can equal a function of θ if and only if both are equal to a common separation constant, which we call λ. The partial differential equation thus splits into a pair of ordinary differential equations

$$r^2\, v'' + r\, v' - \lambda\, v = 0, \qquad\qquad w'' + \lambda\, w = 0, \tag{15.33}$$

that will prescribe the separable solution (15.32). Observe that both have the form of eigenfunction equations in which the separation constant λ plays the role of the eigenvalue, and we are only interested in nonzero solutions or eigenfunctions.

We have already solved the eigenvalue problem for $w(\theta)$. According to (15.31), $w(\theta + 2\,\pi) = w(\theta)$ must be a $2\,\pi$ periodic function. Therefore, according the discussion in Section 12.1, this periodic boundary value problem has the nonzero eigenfunctions

$$1, \qquad \sin n\,\theta, \qquad \cos n\,\theta, \qquad \text{for} \qquad n = 1, 2, \dots . \tag{15.34}$$

corresponding to the eigenvalues (separation constants) $\lambda = n^2$, where $n = 0, 1, 2, \dots$. Fixing the value of λ, the remaining ordinary differential equation

$$r^2 v'' + r\, v' - n^2 v = 0 \tag{15.35}$$

has the form of a second order Euler equation for the radial component $v(r)$. As discussed in Example 7.35, its solutions are obtained by substituting the power ansatz $v(r) = r^k$. We discover that this is a solution if and only if

$$k^2 - n^2 = 0, \qquad \text{and hence} \qquad k = \pm\, n.$$

Therefore, for $n \neq 0$, we find two linearly independent solutions,

$$v_1(r) = r^n, \qquad v_2(r) = r^{-n}, \qquad n = 1, 2, \dots . \tag{15.36}$$

If $n = 0$, there is an additional logarithmic solution

$$v_1(r) = 1, \qquad v_2(r) = \log r, \qquad n = 0. \tag{15.37}$$

Combining (15.34) and (15.36–37), we produce a complete list of separable polar coordinate solutions to the Laplace equation:

$$\begin{array}{lll} 1, & r^n \cos n\,\theta, & r^n \sin n\,\theta, \\ \log r, & r^{-n} \cos n\,\theta, & r^{-n} \sin n\,\theta, \end{array} \qquad n = 1, 2, 3, \dots . \tag{15.38}$$

Now, the solutions in the top row of (15.38) are continuous (in fact analytic) at the origin, whereas the solutions in the bottom row have singularities as $r \to 0$. The latter are not relevant since we require the solution u to remain bounded and smooth — even at the center of the disk. Thus, we should only use the former to concoct a candidate series solution

$$u(r, \theta) \;=\; \frac{a_0}{2} \;+\; \sum_{n=1}^{\infty} \big(a_n\, r^n \cos n\,\theta + b_n\, r^n \sin n\,\theta \big) \tag{15.39}$$

to the Dirichlet boundary value problem. The coefficients a_n, b_n will be prescribed by the boundary conditions (15.30). Substituting $r = 1$, we find

$$u(1,\theta) \;=\; \frac{a_0}{2} \;+\; \sum_{n=1}^{\infty} \big(a_n \cos n\theta + b_n \sin n\theta \big) = h(\theta).$$

We recognize this as a standard Fourier series for the 2π periodic function $h(\theta)$. Therefore,

$$a_n = \frac{1}{\pi} \int_{-\pi}^{\pi} h(\theta) \cos n\theta \, d\theta, \qquad\qquad b_n = \frac{1}{\pi} \int_{-\pi}^{\pi} h(\theta) \sin n\theta \, d\theta, \tag{15.40}$$

are precisely its Fourier coefficients, cf. (12.28).

Remark: Introducing the complex variable $z = r\, e^{\,\mathrm{i}\,\theta} = x + \mathrm{i}\, y$ allows us to write

$$z^n = r^n\, e^{\,\mathrm{i}\, n\theta} = r^n \cos n\theta + \mathrm{i}\, r^n \sin n\theta. \tag{15.41}$$

Therefore, the non-singular separable solutions are nothing but the *harmonic polynomials* we first found in Example 7.52, namely

$$r^n \cos n\theta = \operatorname{Re} z^n, \qquad\qquad r^n \sin n\theta = \operatorname{Im} z^n. \tag{15.42}$$

Exploitation of the remarkable connections between the solutions to the Laplace equation and complex functions will form the focus of Chapter 16.

In view of (15.42), the n^{th} order term in the series solution (15.39),

$$a_n\, r^n \cos n\theta + b_n\, r^n \sin n\theta = a_n \operatorname{Re} z^n + b_n \operatorname{Im} z^n = \operatorname{Re} \big[\, (a_n - \mathrm{i}\, b_n)\, z^n \, \big],$$

is, in fact, a homogeneous polynomial in (x, y) of degree n. This means that, when written in rectangular coordinates x and y, (15.39) is, in fact, a *power series* for the function $u(x, y)$. Proposition C.4 implies that the power series is, in fact, the *Taylor series* for $u(x, y)$ based at the origin, and so its coefficients are multiples of the derivatives of u at $x = y = 0$. Details are worked out in Exercise ■. Thus, the fact that $u(x, y)$ has a convergent Taylor series implies that it is an analytic function at the origin. Indeed, as we will see, analyticity holds at any point of the domain of definintion of a harmonic function .

Example 15.5. Consider the Dirichlet boundary value problem on the unit disk with

$$u(1,\theta) = \theta \qquad \text{for} \qquad -\pi < \theta < \pi. \tag{15.43}$$

The boundary data can be interpreted as a wire in the shape of a single turn of a spiral helix sitting over the unit circle, with a jump discontinuity, of magnitude 2π, at $(-1, 0)$. The required Fourier series

$$h(\theta) = \theta \;\sim\; 2 \left(\sin\theta - \frac{\sin 2\theta}{2} + \frac{\sin 3\theta}{3} - \frac{\sin 4\theta}{4} + \cdots \right)$$

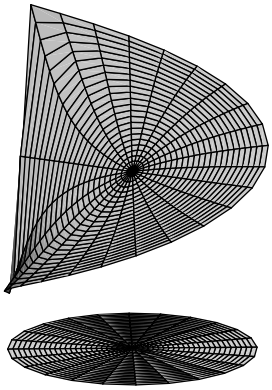

Figure 15.4. Membrane Attached to a Helical Wire.

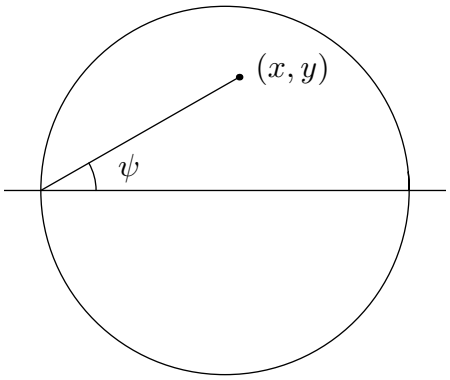

Figure 15.5. Geometrical Construction of the Solution.

was computed in Example 12.2. Therefore, invoking our solution formula (15.39–40),

$$u(r,\theta) = 2\left(r\sin\theta - \frac{r^2\sin 2\theta}{2} + \frac{r^3\sin 3\theta}{3} - \frac{r^4\sin 4\theta}{4} + \cdots\right) \tag{15.44}$$

is the desired solution, and is plotted in Figure 15.4. In fact, this series can be explicitly summed. In view of (15.42),

$$u = 2\ \mathrm{Im}\left(z - \frac{z^2}{2} + \frac{z^3}{3} - \frac{z^4}{4} + \cdots\right) = 2\ \mathrm{Im}\ \log(1+z) = 2\ \mathrm{ph}(1+z) = 2\,\psi, \tag{15.45}$$

where

$$\psi = \tan^{-1}\frac{y}{1+x} \tag{15.46}$$

is the angle that the line passing through the two points (x, y) and $(-1, 0)$ makes with the x-axis, as sketched in Figure 15.5. You should try to convince yourself that, on the unit

circle, $2\psi = \theta$ has the correct boundary values. Obserfve that, even though the boundary values are discontinuous, the solution is an analytic function inside the disk.

Unlike the rectangular series solution (15.23), the polar series solution (15.39) can, in fact, be summed in closed form! If we substitute the explicit Fourier formulae (15.40) into (15.39) — remembering to change the integration variable to, say, ϕ to avoid a notational conflict — we find

$$\begin{aligned} u(r,\theta) &= \frac{a_0}{2} + \sum_{n=1}^{\infty} \big(a_n r^n \cos n\theta + b_n r^n \sin n\theta \big) \\ &= \frac{1}{2\pi} \int_{-\pi}^{\pi} h(\phi)\, d\phi \\ &\qquad + \sum_{n=1}^{\infty} \left[\frac{r^n \cos n\theta}{\pi} \int_{-\pi}^{\pi} h(\phi) \cos n\phi \, d\phi + \frac{r^n \sin n\theta}{\pi} \int_{-\pi}^{\pi} h(\phi) \sin n\phi \, d\phi \right] \\ &= \frac{1}{\pi} \int_{-\pi}^{\pi} h(\phi) \left[\frac{1}{2} + \sum_{n=1}^{\infty} r^n \big(\cos n\theta \cos n\phi + \sin n\theta \sin n\phi \big) \right] d\phi \\ &= \frac{1}{\pi} \int_{-\pi}^{\pi} h(\phi) \left[\frac{1}{2} + \sum_{n=1}^{\infty} r^n \cos n(\theta - \phi) \right] d\phi. \end{aligned} \tag{15.47}$$

We next show how to sum the final series. Using (15.41), we can write it as the real part of a geometric series:

$$\begin{aligned} &\frac{1}{2} + \sum_{n=1}^{\infty} r^n \cos n\theta = \operatorname{Re} \left(\frac{1}{2} + \sum_{n=1}^{\infty} z^n \right) = \operatorname{Re} \left(\frac{1}{2} + \frac{z}{1-z} \right) = \operatorname{Re} \left(\frac{1+z}{2(1-z)} \right) \\ &= \operatorname{Re} \left(\frac{(1+z)(1-\overline{z})}{2\,|\,1-z\,|^2} \right) = \frac{\operatorname{Re}(1+z-\overline{z}-|\,z\,|^2)}{2\,|\,1-z\,|^2} = \frac{1-|\,z\,|^2}{2\,|\,1-z\,|^2} = \frac{1-r^2}{2(1+r^2-2r\cos\theta)}\,. \end{aligned}$$

Substituting back into (15.47) leads to the important *Poisson Integral Formula* for the solution to the boundary value problem.

Theorem 15.6. *The solution to the Laplace equation in the unit disk subject to Dirichlet boundary conditions $u(1,\theta) = h(\theta)$ is*

$$u(r,\theta) = \frac{1}{2\pi} \int_{-\pi}^{\pi} h(\phi)\, \frac{1-r^2}{1+r^2-2\,r\cos(\theta-\phi)}\, d\phi. \tag{15.48}$$

Example 15.7. A particularly important case is when the boundary value

$$h(\theta) = \delta(\theta - \phi)$$

is a delta function concentrated at the point $(\cos\phi, \sin\phi)$, $-\pi < \phi \le \pi$, on the unit circle. The solution to the resulting boundary value problem is the *Poisson integral kernel*

$$u(r,\theta) = \frac{1-r^2}{2\pi\big[\,1+r^2-2\,r\cos(\theta-\phi)\,\big]} = \frac{1-|\,z\,|^2}{2\pi\,|\,1-z\,e^{-\,\mathrm{i}\,\phi}\,|^2}\,. \tag{15.49}$$

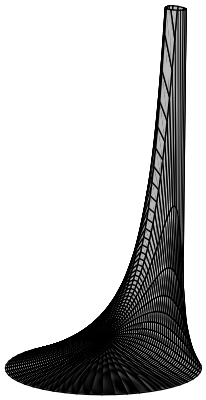

Figure 15.6. The Poisson Kernel.

The reader may enjoy verifying that this function does indeed, solve the Laplace equation and has the correct boundary values in the limit as $r \to 1$. Physically, if $u(r, \theta)$ represents the equilibrium temperature of the disk, then the delta function boundary data correspond to a concentrated unit heat source applied to a single point on the boundary. The resulting solution is sketched in Figure 15.6. Thus, the Poisson kernel plays the role of the fundamental solution for the boundary value problem. Indeed, Poisson integral formula (15.48) follows from our general superposition principle, writing the boundary data as a superposition of delta functions:

$$h(\theta) = \int_{-\pi}^{\pi} h(\phi)\, \delta(\phi - \theta)\, d\phi,$$

Averaging and the Maximum Principle

If we set $r = 0$ in the Poisson formula (15.48), then we obtain

$$u(0, \theta) = \frac{1}{2\,\pi} \int_{-\pi}^{\pi} h(\phi)\, d\phi. \tag{15.50}$$

The left hand side is the value of u at the origin — the center of the disk; the right hand side is the average of its boundary values around the unit circle. This is a particular instance of an important general fact.

Theorem 15.8. *Let $u(x, y)$ be harmonic inside a disk of radius a centered at a point (x_0, y_0) with piecewise continuous (or, more generally, integrable) boundary values on the circle $C = \{\, (x - x_0)^2 + (y - y_0)^2 = a^2 \,\}$. Then its value at the center of the disk is equal to the average of its values on the boundary circle*:

$$u(x_0, y_0) = \frac{1}{2\,\pi\, a} \oint_C u\, ds = \frac{1}{2\,\pi} \int_0^{2\,\pi} u(x_0 + a\cos\theta, y_0 + a\sin\theta)\, d\theta. \tag{15.51}$$

Proof: We use the scaling and translation symmetries of the Laplace equation to map the disk of radius r centered at (x_0, y_0) to the unit disk centered at the origin. Specifically, we set

$$U(x, y) = u(x_0 + a\,x, y_0 + a\,y). \tag{15.52}$$

An easy chain rule computation proves that $U(x,y)$ is harmonic on the unit disk, with boundary values

$$h(\theta) = U(\cos\theta, \sin\theta) = u(x_0 + a\cos\theta, y_0 + a\sin\theta).$$

Therefore, by (15.50) ,

$$U(0,0) = \frac{1}{2\,\pi}\int_{-\pi}^{\pi} h(\theta)\,d\theta = \frac{1}{2\,\pi}\int_{-\pi}^{\pi} U(\cos\theta, \sin\theta)\,d\theta.$$

Replacing U by its formula (15.52) produces the desired result. *Q.E.D.*

An important consequence of the integral formula (15.51) is the *Maximum Principle* for harmonic functions.

Theorem 15.9. *If u is a nonconstant harmonic function defined on a domain Ω, then u does not have a local maximum or local minimum at any interior point of Ω.*

Proof: The average of a continuous real function lies strictly between its maximum and minimum values — except in the trivial case when the function is constant. Since u is harmonic, it is continuous inside Ω. So Theorem 15.8 implies that the value of u at (x,y) lies strictly between its maximal and minimal values on any small circle centered at (x,y). This clearly excludes the possibility of u having a local maximum or minimum at (x,y). *Q.E.D.*

Thus, on a bounded domain, a harmonic function achieves its maximum and minimum values only at boundary points. Any interior critical point, where $\nabla u = \mathbf{0}$, must be a saddle point. Physically, if we interpret $u(x,y)$ as the vertical displacement of a membrane, then Theorem 15.9 says that, in the absence of external forcing, the membrane cannot have any internal bumps — its highest and lowest points are necessarily on the boundary of the domain. This reconfirms our physical intuition: the restoring force exerted by the stretched membrane will serve to flatten any bump, and hence a membrane with a local maximum or minimum cannot be in equilibrium. A similar interpretation holds for heat conduction. A body in thermal equilibrium can achieve its maximum and minimum temperature only on the boundary of the domain. Again, physically, heat energy would flow away from any internal maximum, or towards any local minimum, and so if the body contained a local maximum or minimum on its interior, it could not be in thermal equilibrium.

This concludes our discussion of separation of variables for the planar Laplace equation. The method works in a few other special coordinate systems. See Exercise ■ for one example, and [**131**, **134**, **136**] for a complete account, including connections with the underlying symmetries of the equation.

15.3. The Green's Function.

Now we turn to the Poisson equation (15.3), which is the inhomogeneous form of the Laplace equation. In Section 11.2, we learned how to solve one-dimensional inhomogeneous boundary value problems by contructing the associated Green's function. This important technique can be adapted to solve inhomogeneous boundary value problems for elliptic

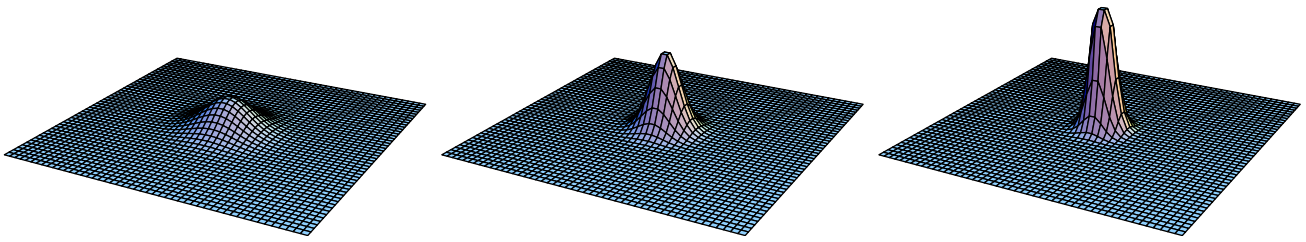

Figure 15.7. Gaussian Distributions Converging to the Delta Function.

partial differential equations in higher dimensions, including Poisson's equation. As before, the Green's function is characterized as the solution to the homogeneous boundary value problem in which the inhomogeneity is a concentrated unit impulse — a delta function. The solution to the general forced boundary value problem is then obtained via linear superposition, that is, as a convolution integral with the Green's function.

The first order of business is to establish the proper form for a unit impulse in our two-dimensional situation. We denote the *delta function* concentrated at position $\boldsymbol{\xi} = (\xi, \eta) \in \mathbb{R}^2$ by

$$\delta_{\boldsymbol{\xi}}(\mathbf{x}) = \delta_{(\xi,\eta)}(x, y) = \delta(\mathbf{x} - \boldsymbol{\xi}). \tag{15.53}$$

The delta function $\delta_{\mathbf{0}}(\mathbf{x}) = \delta(x, y)$ at the origin can be viewed as the limit, as $n \to \infty$, of a sequence of more and more highly concentrated functions $g_n(x, y)$, with

$$\lim_{n \to \infty} g_n(x, y) = 0, \quad \text{for} \quad (x, y) \neq (0, 0), \qquad \text{while} \qquad \iint_\Omega g_n(x, y)\, dx\, dy = 1.$$

A good example of a suitable sequence is provided by the *radial Gaussian distributions*

$$g_n(x, y) = \frac{n}{\pi}\, e^{-n\,(x^2+y^2)}\,, \tag{15.54}$$

which relies on the fact that

$$\iint_{\mathbb{R}^2} e^{-n\,(x^2+y^2)}\, dx\, dy = \frac{\pi}{n}\,,$$

established in Exercise A.6.6. As plotted in Figure 15.7, as $n \to \infty$, the Gaussian profiles become more and more concentrated at the origin, while maintaining a unit volume underneath their graphs.

Alternatively, one can assign the delta function a dual interpretation as a linear functional on the vector space of continuous scalar-valued functions. We formally prescribe the delta function by the integral formula

$$\langle\, \delta_{(\xi,\eta)}\,;\, f\,\rangle = \iint_\Omega \delta_{(\xi,\eta)}(x, y) f(x, y)\, dx\, dy = \begin{cases} f(\xi, \eta), & (\xi, \eta) \in \Omega, \\ 0, & (\xi, \eta) \notin \overline{\Omega}, \end{cases} \tag{15.55}$$

which holds for any continuous function $f(x, y)$ and any domain $\Omega \subset \mathbb{R}^2$. As in the one-dimensional situation, we will avoid defining the integral when the delta function is concentrated at a boundary point, $(\xi, \eta) \in \partial\Omega$, of the integration domain.

Since double integrals can be evaluated as repeated one-dimensional integrals, we can conveniently view

$$\delta_{(\xi,\eta)}(x,y) = \delta_\xi(x)\,\delta_\eta(y) = \delta(x-\xi)\,\delta(y-\eta) \tag{15.56}$$

as the product of a pair of one-dimensional delta functions. Indeed, if

$$(\xi,\eta) \in R = \big\{\, a < x < b,\ c < y < d \,\big\} \subset \Omega$$

is contained in a rectangle inside the domain Ω, then

$$\begin{aligned}\iint_\Omega \delta_{(\xi,\eta)}(x,y) f(x,y)\,dx\,dy &= \iint_R \delta_{(\xi,\eta)}(x,y) f(x,y)\,dx\,dy \\ &= \int_a^b \int_a^b \delta(x-\xi)\,\delta(y-\eta)\,f(x,y)\,dy\,dx = \int_a^b \delta(x-\xi)\,f(x,\eta)\,dx = f(\xi,\eta).\end{aligned}$$

To find the Green's function, we must solve the equilibrium equation subject to a concentrated unit delta force at a prescribed point $\boldsymbol{\xi} = (\xi,\eta) \in \Omega$ inside the domain. In the case of Poisson's equation, the partial differential equation takes the form

$$-\Delta u = \delta_{\boldsymbol{\xi}}, \qquad \text{or} \qquad -\frac{\partial^2 u}{\partial x^2} - \frac{\partial^2 u}{\partial y^2} = \delta(x-\xi)\,\delta(y-\eta), \qquad (x,y) \in \Omega, \tag{15.57}$$

and the solution is subject to homogeneous boundary conditions, either Dirichlet or mixed. (The nonuniqueness of solutions to the pure Neumann boundary value problem precludes the existence of a Green's function.) The resulting solution to the Poisson boundary value problem is denoted as

$$G(\mathbf{x};\boldsymbol{\xi}) = G(x,y;\xi,\eta), \tag{15.58}$$

and called the *Green's function*. Thus, the Green's function (15.58) measures the effect, at position $\mathbf{x} = (x,y)$, of a concentrated force applied at position $\boldsymbol{\xi} = (\xi,\eta)$.

Once we know the Green's function, the solution to the general Poisson boundary value problem

$$-\Delta u = f \qquad \text{in} \qquad \Omega, \qquad\qquad u = 0 \qquad \text{on} \qquad \partial\Omega \tag{15.59}$$

is reconstructed through a superposition principle. We regard the forcing function

$$f(x,y) = \iint_\Omega \xi\eta\delta(x-\xi)\,\delta(y-\eta) f(\xi,\eta)$$

as a superposition of delta impulses, whose strength at each point equals the value of f there. Linearity implies that the solution to the boundary value problem is the corresponding superposition of Green's function responses to each of the constituent impulses. The net result is the fundamental *superposition formula*

$$u(x,y) = \iint_\Omega \xi\eta G(x,y;\xi,\eta)\,f(\xi,\eta) \tag{15.60}$$

for the solution. This can be verified by direct evalution:

$$\begin{aligned} -\Delta u(x,y) &= \iint_\Omega \xi\eta[-\Delta G(x,y;\xi,\eta)]\, f(\xi,\eta) \\ &= \iint_\Omega \xi\eta\delta(x-\xi,y-\eta)\, f(\xi,\eta) = f(x,y), \end{aligned}$$

as claimed.

As in the one-dimensional situation, self-adjointness of the boundary value problem is manifested in the symmetry of the Green's function under interchange of its arguments:

$$G(\xi,\eta;x,y) = G(x,y;\xi,\eta). \tag{15.61}$$

The general proof of symmetry follows as in the one-dimensional version (11.91); see Exercise ■. Symmetry has the following intriguing physical interpretation: Let $\mathbf{x}, \boldsymbol{\xi} \in \Omega$ be any pair of points in the domain. We apply a unit impulse to the membrane at the first point, and measure its deflection at the second; the result is exactly the same as if we apply the impulse at the second point, and measure the deflection at the first! (On the other hand, the deflections at other points in the domain will typically bear very little connection with each other.) Similarly, in electrostatics, the solution $u(x,y)$ is interpreted as the electrostatic potential for a system in equilibrium. A delta function corresponds to a point charge, e.g., an electron. The symmetry property says that the electrostatic potential at $\mathbf{x}$ due to a point charge placed at position $\boldsymbol{\xi}$ is exactly the same as the potential at $\boldsymbol{\xi}$ due to a point charge at $\mathbf{x}$. The reader may wish to meditate on the physical plausibility of these remarkable facts.

Unfortunately, most Green's functions — with a few notable exceptions — cannot be written down in closed form. However, their intrinsic form can be based on the following construction. Let us begin by considering the solution to the required Poisson equation

$$-\Delta u = \delta(x-\xi,y-\eta) \tag{15.62}$$

where $(\xi,\eta) \in \Omega$ is the point that the unit impulse force is being applied. As usual, the general solution to an inhomogeneous linear equation is a sum

$$u(x,y) = u_\star(x,y) + z(x,y) \tag{15.63}$$

of a particular solution $u_\star$ combined with the general solution z to the corresponding homogeneous equation, namely

$$-\Delta z = 0.$$

That is, $z(x,y)$ is an arbitrary harmonic function. We shall assume that the particular solution $u_\star(x,y)$ is due to the effect of the unit impulse, irrespective of any imposed boundary conditions. Once we have determined $u_\star$, we shall use the freedom inherent in the harmonic constituent $z(x,y)$ to ensure that the sum (15.63) satisfies the required boundary conditions.

One way to find a particular solution $u_\star$ is to appeal to physical intuition. First, since the delta function is concentrated at the point $\boldsymbol{\xi}$, the solution $u_\star$ must solve the homogeneous Laplace equation $\Delta u_\star = 0$ except at the point $\mathbf{x} = \boldsymbol{\xi}$, where we expect

it to have some sort of discontinuity. Second, since the Poisson equation is modeling a homogeneous, uniform medium (membrane, plate, gravitational potential in empty space, etc.), in the absence of boundary conditions, the effect of a unit impulse should only depend upon on the distance away from the source of the impulse. Therefore, we expect that the desired particular solution will depend only on the radial variable:

$$u_\star = u_\star(r), \qquad \text{where} \qquad r = \| \mathbf{x} - \boldsymbol{\xi} \| = \sqrt{(x-\xi)^2 + (y-\eta)^2}\,.$$

According to (15.37), the only radially symmetric solutions to the Laplace equation are

$$u(r) = a + b \log r, \tag{15.64}$$

where a and b are constants. The constant term a is smooth and harmonic everywhere, and so cannot contribute to a delta function singularity. Therefore, our only chance to produce a solution with such a singularity at the point $\boldsymbol{\xi}$ is to take a multiple of the logarithmic potential:

$$u_\star = b \, \log r.$$

We claim that, modulo the determination of b, this gives the correct formula, so

$$-\Delta u_\star = -b\,\Delta(\log r) = \delta(\mathbf{x} - \boldsymbol{\xi}), \qquad r = \| \mathbf{x} - \boldsymbol{\xi} \|. \tag{15.65}$$

is the delta function for an appropriate constant b.

To justify this claim, and so determine the proper value of b, we first note that, by construction, $\log r$ solves the Laplace equation everywhere except at $r = 0$, i.e., at $\mathbf{x} = \boldsymbol{\xi}$:

$$\Delta \log r = 0, \qquad r \neq 0. \tag{15.66}$$

Secondly, if $D_a = \big\{\, 0 \leq r \leq a \,\big\} = \big\{\, \| \mathbf{x} - \boldsymbol{\xi} \| \leq a \,\big\}$ is any disk centered at $\boldsymbol{\xi}$, then, by the divergence form (A.60) of Green's Theorem,

$$\begin{aligned} \iint_{D_a} \Delta(\log r)\, dx\, dy &= \iint_{D_a} \nabla \cdot \nabla(\log r)\, dx\, dy \\ &= \oint_{C_a} \frac{\partial(\log r)}{\partial \mathbf{n}}\, ds = \oint_{C_a} \frac{\partial(\log r)}{\partial r}\, ds = \oint_{C_a} \frac{1}{r}\, ds = \int_{-\pi}^{\pi} d\theta = 2\,\pi, \end{aligned}$$

where $C_a = \partial D_a = \big\{\, \| \mathbf{x} - \boldsymbol{\xi} \| = a \,\big\}$ is the boundary of the disk, i.e., the circle of radius a centered at $\boldsymbol{\xi}$. (The identification $\partial/\partial \mathbf{n} = \partial/\partial r$ on a circle can be found in Exercise A.7.7.) Thus, if Ω is any domain, then

$$\iint_{\Omega} \Delta(\log r)\, dx\, dy = \begin{cases} 2\,\pi, & \boldsymbol{\xi} \in \Omega, \\ 0, & \boldsymbol{\xi} \notin \overline{\Omega}. \end{cases} \tag{15.67}$$

In the first case, when $\boldsymbol{\xi} \in \Omega$, (15.66) allows us replace the integral over Ω by an integral over a small disk centered at $\boldsymbol{\xi}$, and then apply the preceding identity; in the second case, (15.68) implies that the integrand vanishes on all of the domain, and so the integral is 0. Equations (15.66–67) are the defining properties for $2\,\pi$ times the delta function, so

$$\Delta(\log r) = 2\,\pi\,\delta(\mathbf{x} - \boldsymbol{\xi}). \tag{15.68}$$

Comparing (15.68) with (15.65), we conclude that

$$u_\star(x,y) = -\frac{1}{2\pi}\,\log r = -\frac{1}{2\pi}\log\|\,\mathbf{x}-\boldsymbol{\xi}\,\| = -\frac{1}{4\pi}\log\big[\,(x-\xi)^2+(y-\eta)^2\,\big] \qquad (15.69)$$

is a particular solution to the Poisson equation (15.62) with a unit impulse force.

The *logarithmic potential* (15.69) represents the gravitational potential in empty two-dimensional space due to a unit point mass at position $\boldsymbol{\xi}$, or, equivalently, the two-dimensional electrostatic potential due to a point charge at $\boldsymbol{\xi}$. The corresponding gravitational (electrostatic) force field is obtained by taking its gradient:

$$\mathbf{F} = \nabla\left(-\frac{1}{2\pi}\log\|\,\mathbf{x}-\boldsymbol{\xi}\,\|\right) = -\frac{\mathbf{x}-\boldsymbol{\xi}}{2\pi\,\|\,\mathbf{x}-\boldsymbol{\xi}\,\|^2}\,.$$

Note that $\|\,\mathbf{F}\,\| = 1/(2\pi\,\|\,\mathbf{x}-\boldsymbol{\xi}\,\|)$ is proportional to the inverse distance, which is the two-dimensional form of Newton's (Coulomb's) three-dimensional inverse square law. The gravitational potential due to a mass, e.g., a plate, in the shape of a domain $\Omega \subset \mathbb{R}^2$ can be obtained by superimposing delta function sources with strengths equalo to the density of the material at each point. The result is the potential function

$$u(x,y) = -\frac{1}{4\pi}\iint_\Omega \xi\eta\rho(\xi,\eta)\,\log\big[\,(x-\xi)^2+(y-\eta)^2\,\big]\,d\xi\,d\eta, \qquad (15.70)$$

in which $\rho(\xi,\eta)$ denotes the density of the body at position (ξ,η). For example, the gravitational potential due to the unit disk $D = \{\,x^2+y^2 \le 1\,\}$ with unit density $\rho \equiv 1$ is

$$u(x,y) = -\frac{1}{4\pi}\iint_D \xi\eta\log\big[\,(x-\xi)^2+(y-\eta)^2\,\big]\,.$$

Returning to our boundary value problem, the general solution to the Poisson equation (15.62) can, therefore, be written in the form

$$u(x,y) = -\frac{1}{2\pi}\,\log\|\,\mathbf{x}-\boldsymbol{\xi}\,\| + z(x,y), \qquad (15.71)$$

where $z(x,y)$ is an arbitrary harmonic function. To construct the Green's function for a prescribed domain, we need to choose the harmonic function $z(x,y)$ so that (15.71) satisfies the relevant homogeneous boundary conditions. Let us state this result for the Dirichlet problem.

Proposition 15.10. *The Green's function for the Dirichlet boundary value problem*

$$-\Delta u = f \qquad \text{on} \qquad \Omega, \qquad\qquad u = 0 \qquad \text{on} \qquad \partial\Omega,$$

has the form

$$G(x,y;\xi,\eta) = -\frac{1}{4\pi}\,\log\big[\,(x-\xi)^2+(y-\eta)^2\,\big] + z(x,y) \qquad (15.72)$$

where $z(x,y)$ is the harmonic function that has the same boundary values as the logarithmic potential function:

$$\Delta z = 0 \quad \text{on} \quad \Omega, \qquad\qquad z(x,y) = \frac{1}{4\pi}\,\log\big[\,(x-\xi)^2+(y-\eta)^2\,\big] \quad \text{for} \quad (x,y)\in\partial\Omega.$$

Let us conclude this subsection by summarizing the key properties of the Green's function $G(\mathbf{x}, \boldsymbol{\xi})$ for the two-dimensional Poisson equation., which

(a) Solves Laplace's equation, $\Delta G = 0$, for all $\mathbf{x} \neq \boldsymbol{\xi}$.

(b) Has a logarithmic singularity[†] at $\mathbf{x} = \boldsymbol{\xi}$.

(c) Satisfies the relevant homogeneous boundary conditions.

(d) Is symmetric: $G(\boldsymbol{\xi}, \mathbf{x}) = G(\mathbf{x}, \boldsymbol{\xi})$.

(e) Establishes the superposition formula (15.60) for a general forcing function.

The Method of Images

The preceding analysis exposes the underlying form of the Green's function, but we are still left with the determination of the harmonic component $z(x, y)$ required to match the logarithmic potential boundary values. There are three principal analytical techniques employed to produce explicit formulas. The first is an adaptation of the method of separation of variables, and leads to infinite series expressions, similar to those of the fundamental solution for the heat equation derived in Chapter 14. We will not dwell on this approach here, although a couple of the exercises ask the reader to fill in the details. The second is the *method of images* and will be developed in this section. The most powerful is based on the theory of conformal mappings, but must be deferred until we have learned the basics of complex analysis; the details can be found in Section 16.3. While the first two methods only apply to a fairly limited class of domains, they do adapt straightforwardly to higher dimensional problems, as well as certain other types of elliptic partial differential equations, whereas the method of conformal mapping is, unfortunately, restricted to two-dimensional problems involving the Laplace and Poisson equations.

We already know that the singular part of the Green's function for the two-dimensional Poisson equation is provided by a logarithmic potential. The problem, then, is to construct the harmonic part, called $z(x, y)$ in (15.72), so that the sum has the correct homogeneous boundary values, or, equivalently, that $z(x, y)$ has the same boundary values as the logarithmic potential. In certain cases, $z(x, y)$ can be thought of as the potential induced by one or more hypothetical electric charges (or, equivalently, gravitational point masses) that are located *outside* the domain Ω, arranged in such a manner that their combined electrostatic potential happens to coincide with the logarithmic potential on the boundary of the domain. The goal, then, is to place the image charges of suitable strength in the proper positions.

Here, we will only consider the case of a single image charge, located at a position $\boldsymbol{\eta} \notin \Omega$. We scale the logarithmic potential (15.69) by the charge strength, and, for added flexibility, include an additional constant — the charge's potential baseline:

$$z(x, y) = a \log \| \mathbf{x} - \boldsymbol{\eta} \| + b, \qquad \eta \in \mathbb{R}^2 \setminus \overline{\Omega}.$$

This function is harmonic inside Ω since the logarithmic potential is harmonic everywhere except at the singularity $\boldsymbol{\eta}$, which is assumed to lies outside the domain. For the Dirichlet

[†] Note that this is in contrast to the one-dimensional situation, where the Green's function is continuous at the impulse point.

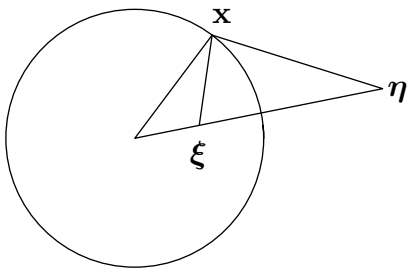

Figure 15.8. Method of Images for the Unit Disk.

boundary value problem, then, for each point $\boldsymbol{\xi} \in \Omega$, we must find a corresponding image point $\boldsymbol{\eta} \in \mathbb{R}^2 \setminus \overline{\Omega}$ and constants $a, b \in \mathbb{R}$, such that[‡]

$$\log \| \mathbf{x} - \boldsymbol{\xi} \| = a \log \| \mathbf{x} - \boldsymbol{\eta} \| + b \qquad \text{for all} \qquad \mathbf{x} \in \partial\Omega,$$

or, equivalently,

$$\| \mathbf{x} - \boldsymbol{\xi} \| = \lambda \| \mathbf{x} - \boldsymbol{\eta} \|^a \qquad \text{for all} \qquad \mathbf{x} \in \partial\Omega, \tag{15.73}$$

where $\lambda = \log b$. For each fixed $\boldsymbol{\xi}, \boldsymbol{\eta}, \lambda, a$, the equation in (15.73) will, typically, implicitly prescribe a plane curve, but it is not clear that one can always arrange that these curves all coincide with the boundary of our domain.

In order to make further progress, we appeal to a geometrical construction based upon similar triangles. We select $\boldsymbol{\eta} = c\,\boldsymbol{\xi}$ to be a point lying on the ray through $\boldsymbol{\xi}$. Its location is fixed so that the triangle with vertices $\mathbf{0}, \mathbf{x}, \boldsymbol{\eta}$ is similar to the triangle with vertices $\mathbf{0}, \boldsymbol{\xi}, \mathbf{x}$, noting that they have the same angle at the common vertex $\mathbf{0}$ — see Figure 15.8. Similarity requires that the triangles' corresponding sides have a common ratio, and so

$$\frac{\| \boldsymbol{\xi} \|}{\| \mathbf{x} \|} = \frac{\| \mathbf{x} \|}{\| \boldsymbol{\eta} \|} = \frac{\| \mathbf{x} - \boldsymbol{\xi} \|}{\| \mathbf{x} - \boldsymbol{\eta} \|} = \lambda. \tag{15.74}$$

The last equality implies that (15.73) holds with $a = 1$. Consequently, if we choose

$$\| \boldsymbol{\eta} \| = \frac{1}{\| \boldsymbol{\xi} \|}, \qquad \text{so that} \qquad \boldsymbol{\eta} = \frac{\boldsymbol{\xi}}{\| \boldsymbol{\xi} \|^2}, \tag{15.75}$$

then

$$\| \mathbf{x} \|^2 = \| \boldsymbol{\xi} \| \, \| \boldsymbol{\eta} \| = 1.$$

Thus $\mathbf{x}$ lies on the unit circle, and, as a result, $\lambda = \| \boldsymbol{\xi} \|$. The map taking a point $\boldsymbol{\xi}$ inside the disk to its image point $\boldsymbol{\eta}$ defined by (15.75) is known as *inversion* with respect to the unit circle.

[‡] To simplify the formulas, we have omitted the $1/(2\pi)$ factor, which can easily be reinstated at the end of the analysis.

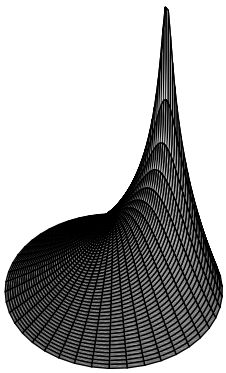

Figure 15.9. Green's Function for the Unit Disk.

We have now demonstrated that the functions

$$\frac{1}{2\pi}\,\log\|\,\mathbf{x}-\boldsymbol{\xi}\,\| = \frac{1}{2\pi}\,\log\big(\,\|\,\boldsymbol{\xi}\,\|\;\|\,\mathbf{x}-\boldsymbol{\eta}\,\|\,\big) = \frac{1}{2\pi}\,\log\frac{\|\,\|\,\boldsymbol{\xi}\,\|^2\,\mathbf{x}-\boldsymbol{\xi}\,\|}{\|\,\boldsymbol{\xi}\,\|} \quad \text{when} \quad \|\,\mathbf{x}\,\| = 1, \tag{15.76}$$

has the same boundary values on the unit circle. Consequently, their difference

$$G(\mathbf{x};\boldsymbol{\xi}) = -\,\frac{1}{2\pi}\log\|\,\mathbf{x}-\boldsymbol{\xi}\,\| + \frac{1}{2\pi}\log\frac{\|\,\|\,\boldsymbol{\xi}\,\|^2\,\mathbf{x}-\boldsymbol{\xi}\,\|}{\|\,\boldsymbol{\xi}\,\|} = \frac{1}{2\pi}\log\frac{\|\,\|\,\boldsymbol{\xi}\,\|^2\,\mathbf{x}-\boldsymbol{\xi}\,\|}{\|\,\boldsymbol{\xi}\,\|\;\|\,\mathbf{x}-\boldsymbol{\xi}\,\|} \tag{15.77}$$

has the required properties for the Green's function for the Dirichlet problem on the unit disk. In terms of polar coordinates

$$\mathbf{x} = (r\cos\theta, r\sin\theta), \qquad \boldsymbol{\xi} = (\rho\cos\varphi, \rho\sin\varphi),$$

applying the Law of Cosines to the triangles in Figure 15.8 leads to the explicit formula

$$G(r,\theta;\rho,\varphi) = \frac{1}{4\pi}\,\log\left(\frac{1+r^2\rho^2-2\,r\,\rho\cos(\theta-\varphi)}{r^2+\rho^2-2\,r\,\rho\cos(\theta-\varphi)}\right). \tag{15.78}$$

In Figure 15.9 we sketch the Green's function corresponding to a unit impulse being applied at a point half way between the center and the edge of the disk.

Remark: Unlike one-dimensional boundary value problems, the Green's function (15.78) has a singularity and is not continuous at the impulse point $\mathbf{x} = \boldsymbol{\xi}$.

Applying the general superposition rule (15.60), we arrive at a solution to the Dirichlet boundary value problem for the Poisson equation in the unit disk.

Theorem 15.11. *The solution to the homogeneous Dirichlet boundary value problem*

$$-\,\Delta u = f, \quad \textit{for} \quad r = \|\,\mathbf{x}\,\| < 1, \qquad\qquad u = 0, \quad \textit{for} \quad r = 1,$$

is, when expressed in polar coordinates,

$$u(r,\theta) = \frac{1}{4\pi}\int_0^{2\pi}\int_0^1 f(\rho,\varphi)\,\log\left(\frac{1+r^2\rho^2-2\,r\,\rho\cos(\theta-\varphi)}{r^2+\rho^2-2\,r\,\rho\cos(\theta-\varphi)}\right)\rho\,d\rho\,d\varphi. \tag{15.79}$$

The Green's function was originally designed for the homogeneous boundary value problem. Interestingly, it can also be used to handle inhomogeneous boundary conditions.

Theorem 15.12. *Let $G(\mathbf{x};\boldsymbol{\xi})$ denote the Green's function for the homogeneous Dirichlet boundary value problem for the Poisson equation on a domain $\Omega \subset \mathbb{R}^2$. Then the solution to the inhomogeneous Dirichlet problem*

$$-\Delta u = f, \qquad \mathbf{x} \in \Omega, \qquad\qquad u = h, \qquad \mathbf{x} \in \partial\Omega, \tag{15.80}$$

is given by

$$u(\mathbf{x}) = \iint_\Omega \xi\eta G(\mathbf{x};\boldsymbol{\xi})\, f(\boldsymbol{\xi}) - \oint_{\partial\Omega} \frac{\partial G(\mathbf{x};\boldsymbol{\xi})}{\partial \mathbf{n}}\, h(\boldsymbol{\xi})\, ds. \tag{15.81}$$

For example, applying (15.81) to the Green's function (15.78) for the unit disk with $f \equiv 0$ recovers the Poisson integral formula (15.48).

Proof: Let $\psi(\mathbf{x})$ be any function such that

$$\psi = h \qquad \text{for} \qquad \mathbf{x} \in \partial\Omega.$$

Set $v = u - \psi$, so that v satisfies the homogeneous boundary value problem

$$-\Delta v = f + \Delta\psi \qquad \text{in} \qquad \Omega, \qquad\qquad v = 0 \qquad \text{on} \qquad \partial\Omega.$$

We can therefore express

$$v(\mathbf{x}) = \iint_\Omega \xi\eta G(\mathbf{x};\boldsymbol{\xi}) \big[\, f(\boldsymbol{\xi}) + \Delta\psi(\boldsymbol{\xi}) \,\big]. \tag{15.82}$$

Integration by parts, based on the second formula in Exercise A.7.6, can be used to simplify the integral:

$$\iint_\Omega G(\mathbf{x};\boldsymbol{\xi})\, \Delta\psi(\boldsymbol{\xi})\, d\xi\, d\eta = \iint_\Omega \xi\eta \Delta G(\mathbf{x};\boldsymbol{\xi})\, \psi(\boldsymbol{\xi}) + \\ + \oint_{\partial\Omega} \left(G(\mathbf{x};\boldsymbol{\xi})\, \frac{\partial\psi(\boldsymbol{\xi})}{\partial \mathbf{n}} - \frac{\partial G(\mathbf{x};\boldsymbol{\xi})}{\partial \mathbf{n}}\, \psi(\boldsymbol{\xi}) \right) ds.$$

Since the Green's function solves $-\Delta G = \delta_{\boldsymbol{\xi}}$, the first term reproduces $-\psi(\mathbf{x})$. Moreover, $G = 0$ and $\psi = h$ on $\partial\Omega$, and so the right hand side of (15.82) reduces to the desired formula (15.81). *Q.E.D.*

15.4. Adjoints and Minimum Principles.

In this section, we explain how the Laplace and Poisson equations fit into our universal self-adjoint equilibrium framework. The most important outcome will be to establish a very famous minimization principle characterizing the equilibrium solution, that we will exploit in the design of the finite element numerical solution method.

The one-dimensional version of the Poisson equation,

$$-\frac{d^2u}{dx^2} = f,$$

is the equilibrium equation for a uniform elastic bar. In Section 11.3, we wrote the underlying boundary value problems in self-adjoint form

$$K[u] = D^* \circ D[u] = f$$

based on the product of the derivative operator $Du = u'$ and its adjoint $D^* = -D$ with respect to the standard L^2 inner product.

For the two-dimensional Poisson equation

$$-\Delta[u] = -\frac{\partial^2 u}{\partial x^2} - \frac{\partial^2 u}{\partial y^2} = f(x,y)$$

the role of the one-dimensional derivative D will be played by the *gradient* operator

$$\nabla u = \operatorname{grad} u = \begin{pmatrix} u_x \\ u_y \end{pmatrix}.$$

The gradient ∇ defines a linear map that takes a scalar-valued function $u(x,y)$ to the vector-valued function consisting of its two first order partial derivatives. Thus, its domain is the vector space $U = \mathrm{C}^1(\Omega, \mathbb{R})$ consisting of all continuously differentiable functions $u(x,y)$ defined for $(x,y) \in \Omega$. The target space $V = \mathrm{C}^0(\Omega, \mathbb{R}^2)$ consists of all continuous vector-valued functions $\mathbf{v}(x,y) = \big(\, v_1(x,y), v_2(x,y) \,\big)^T$, also known as *vector fields*. (By way of analogy, scalar-valued functions are sometimes referred to as *scalar fields*.) Indeed, if $u_1, u_2 \in U$ are any two scalar functions and $c_1, c_2 \in \mathbb{R}$ any constants, then

$$\nabla(c_1\, u_1 + c_2\, u_2) = c_1\, \nabla u_1 + c_2\, \nabla u_2,$$

which is the requirement for linearity as stated in Definition 7.1.

In accordance with the general Definition 7.53, the adjoint of the gradient must go in the reverse direction,

$$\nabla^* \colon V \longrightarrow U,$$

mapping vector fields $\mathbf{v}(x,y)$ to scalar functions $z(x,y) = \nabla^* \mathbf{v}$. The defining equation for the adjoint

$$\langle\!\langle\, \nabla u \,;\, \mathbf{v} \,\rangle\!\rangle = \langle\, u \,;\, \nabla^* \mathbf{v} \,\rangle \tag{15.83}$$

depends on the choice of inner products on the two vector spaces. The simplest inner product between real-valued scalar functions $u(x,y), \widetilde{u}(x,y)$ defined on a domain $\Omega \subset \mathbb{R}^2$ is given by the double integral

$$\langle\, u \,;\, \widetilde{u} \,\rangle = \iint_\Omega u(x,y)\, \widetilde{u}(x,y)\, dx\, dy. \tag{15.84}$$

As in the one-dimensional case (3.12), this is often referred to as the L^2 *inner product* between scalar fields, with associated norm

$$\| u \| = \sqrt{\langle\, u \,;\, u \,\rangle} = \sqrt{\iint_\Omega u(x,y)^2\, dx\, dy}\,.$$

Similarly, the L^2 inner product between vector-valued functions (vector fields) defined on Ω is obtained by integrating their usual dot product:

$$\langle\!\langle\, \mathbf{v}\,;\widetilde{\mathbf{v}}\,\rangle\!\rangle = \iint_\Omega \mathbf{v}(x,y)\cdot\widetilde{\mathbf{v}}(x,y)\,dx\,dy = \iint_\Omega \big[\, v_1(x,y)\,\widetilde{v}_1(x,y) + v_2(x,y)\,\widetilde{v}_2(x,y)\,\big]\,dx\,dy. \tag{15.85}$$

These form the two most basic inner products on the spaces of scalar and vector fields, and are the ones required to place the Laplace and Poisson equations in self-adjoint form.

The adjoint identity (15.83) is supposed to hold for all appropriate scalar fields u and vector fields $\mathbf{v}$. For the L^2 inner products (15.84, 85), the two sides of the identity read

$$\langle\!\langle\, \nabla u\,;\mathbf{v}\,\rangle\!\rangle = \iint_\Omega \nabla u\cdot\mathbf{v}\,dx\,dy = \iint_\Omega \left(\frac{\partial u}{\partial x}\,v_1 + \frac{\partial u}{\partial y}\,v_2\right) dx\,dy,$$
$$\langle\, u\,;\nabla^*\mathbf{v}\,\rangle = \iint_\Omega u\,\nabla^*\mathbf{v}\,dx\,dy.$$

Thus, to equate these two double integrals, we must soomehow remove the derivatives from the scalar field u. As in the one-dimensional computation (11.74), the secret is integration by parts.

For single integrals, the integration by parts formula is found by applying the Fundamental Theorem of Calculus to Leibniz's rule for the derivative of the product of two functions. According to Appendix A, Green's Theorem A.26 plays the role of the Fundamental Theorem when dealing with double integrals. We will find the divergence form

$$\iint_\Omega \nabla\cdot\mathbf{v}\,dx\,dy = \oint_{\partial\Omega} \mathbf{v}\cdot\mathbf{n}\,ds, \tag{15.86}$$

as in (A.60), the more convenient for the present purposes. Proceeding in analogy with the one-dimensional argument, we replace the vector field $\mathbf{v}$ by the product $u\,\mathbf{v}$ of a scalar field u and a vector field $\mathbf{v}$. An elementary computation proves that

$$\nabla\cdot(u\,\mathbf{v}) = u\,\nabla\cdot\mathbf{v} + \nabla u\cdot\mathbf{v}. \tag{15.87}$$

As a result, we deduce what is usually known as *Green's formula*

$$\iint_\Omega \big[\, u\,\nabla\cdot\mathbf{v} + \nabla u\cdot\mathbf{v}\,\big]\,dx\,dy = \oint_{\partial\Omega} u\,(\mathbf{v}\cdot\mathbf{n})\,ds, \tag{15.88}$$

which is valid for arbitrary bounded domains Ω, and arbitrary scalar and vector fields defined thereon. Rearranging the terms in this integral identity produces the required *integration by parts* formula for double integrals:

$$\iint_\Omega \nabla u\cdot\mathbf{v}\,dx\,dy = \oint_{\partial\Omega} u\,(\mathbf{v}\cdot\mathbf{n})\,ds - \iint_\Omega u\,\nabla\cdot\mathbf{v}\,dx\,dy. \tag{15.89}$$

The terms in this identity have direct counterparts in our one-dimensional integration by parts formula (11.77). The first term on the right hand side of this identity is a boundary term, just like the first terms on the right hand side of the one-dimensional formula (11.77). Moreover, the derivative operation has moved from a gradient on the scalar field in the

doubl.e integral on the left to a divergence on the vector field in the double integral on the right — even the minus sign is in place!

Now, the left hand side in the integration by parts formula (15.89) is the same as the left hand side of (15.83). If the boundary integral vanishes,

$$\oint_{\partial\Omega} u\,\mathbf{v}\cdot\mathbf{n}\,ds = 0, \tag{15.90}$$

then the right hand side of formula (15.89) also reduces to an L^2 inner product

$$-\iint_\Omega u\,\nabla\cdot\mathbf{v}\,dx\,dy = \iint_\Omega u\,(-\nabla\cdot\mathbf{v})\,dx\,dy = \langle\, u\,;-\nabla\cdot\mathbf{v}\,\rangle$$

between the scalar field u and minus the divergence of the vector field $\mathbf{v}$. Therefore, subject to the boundary constraint (15.90), the integration by parts formula reduces to the inner product identity

$$\langle\!\langle\, \nabla u\,;\mathbf{v}\,\rangle\!\rangle = \langle\, u\,;\,-\nabla\cdot\mathbf{v}\,\rangle. \tag{15.91}$$

Comparing (15.83) with (15.91), we conclude that

$$\nabla^*\mathbf{v} = -\nabla\cdot\mathbf{v}, \tag{15.92}$$

and hence, when subject to the proper boundary conditions, the adjoint of the gradient operator is minus the divergence: $\nabla^* = -\nabla\cdot$. In this manner, we are able to write the two-dimensional Poisson equation in the standard self-adjoint form

$$-\Delta u = \nabla^*\circ\nabla u = -\nabla\cdot(\nabla u) = f \tag{15.93}$$

subject to an appropriate system of boundary conditions that justify (15.91).

The vanishing of the boundary integral (15.90) will be ensured by the imposition of suitable homogeneous boundary conditions on the scalar field u and/or the vector field $\mathbf{v}$. Clearly the line integral will vanish if either $u = 0$ or $\mathbf{v}\cdot\mathbf{n} = 0$ at each point on the boundary. These lead immediately to the three principle types of boundary conditions. The first are the fixed or *Dirichlet boundary conditions*, which require

$$u = 0 \qquad \text{on} \qquad \partial\Omega. \tag{15.94}$$

Alternatively, we can require

$$\mathbf{v}\cdot\mathbf{n} = 0 \qquad \text{on} \qquad \partial\Omega, \tag{15.95}$$

which requires that $\mathbf{v}$ be tangent to $\partial\Omega$ at each point, and so there is no net flux across the (solid) boundary. If we identify $\mathbf{v} = \nabla u$, then the no flux boundary condition (15.95) translates into the *Neumann boundary conditions*

$$\frac{\partial u}{\partial\mathbf{n}} = \nabla u\cdot\mathbf{n} = 0 \qquad \text{on} \qquad \partial\Omega. \tag{15.96}$$

One can evidently also mix the boundary conditions, imposing Dirichlet conditions on part of the boundary, and Neumann on the complementary part:

$$u = 0 \quad \text{on} \quad D, \qquad \frac{\partial u}{\partial\mathbf{n}} = 0 \quad \text{on} \quad N, \qquad \text{where} \qquad \partial\Omega = D\cup N \tag{15.97}$$

is the disjoint union of the Dirichlet and Neumann parts.

More generally, when modeling inhomogeneous membranes, heat flow through inhomogeneous media, and similar physical equilibria, we replace the L^2 inner product between vector fields (15.85) by a weighted version

$$\langle\!\langle\, \mathbf{v}\,;\widetilde{\mathbf{v}}\,\rangle\!\rangle = \iint_\Omega \big[\, p(x,y)\, v_1(x,y)\, \widetilde{v}_1(x,y) + q(x,y)\, v_2(x,y)\, \widetilde{v}_2(x,y)\,\big]\, dx\, dy, \tag{15.98}$$

in which $p(x,y), q(x,y) > 0$ are strictly positive functions on the domain $(x,y) \in \Omega$. These functions are determined by the underlying physical properties of the medium being modeled. Retaining the usual L^2 inner product (15.84) between scalar fields, let us compute the weighted adjoint of the gradient operator, as defined by (15.83). As before, we use the basic integration by parts formula (15.89) to remove the derivatives from the scalar field u, and so

$$\begin{aligned} \langle\!\langle\, \nabla u\,;\mathbf{v}\,\rangle\!\rangle &= \iint_\Omega \left(p\, v_1\, \frac{\partial u}{\partial x} + q\, v_2\, \frac{\partial u}{\partial y} \right) dx\, dy \\ &= \oint_{\partial\Omega} \big(-u\, q\, v_2\, dx + u\, p\, v_1\, dy \big) - \iint_\Omega u \left(\frac{\partial (p\, v_1)}{\partial x} + \frac{\partial (q\, v_2)}{\partial y} \right) dx\, dy. \end{aligned} \tag{15.99}$$

Equating the left hand side to $\langle\, u\,;\nabla^*\mathbf{v}\,\rangle$, we deduce that, provided the boundary integral vanishes, the weighted adjoint of the gradient operator with respect to the inner products (15.84), (15.98) is given by

$$\nabla^*\mathbf{v} = -\,\frac{\partial (p\, v_1)}{\partial x} - \frac{\partial (q\, v_2)}{\partial y} = -\,p\,\frac{\partial v_1}{\partial x} - q\,\frac{\partial v_2}{\partial y} - v_1\,\frac{\partial p}{\partial x} - v_2\,\frac{\partial q}{\partial y}\,. \tag{15.100}$$

This holds provided the scalar and vector fields satisfy suitable boundary conditions; for example, requiring either $u(x,y) = 0$ or $\mathbf{v}(x,y) = 0$ at every boundary point $(x,y) \in \partial\Omega$ will cause the boundary integral in (15.99) to vanish, and hence justify (15.100). As a result, all of the usual homogeneous boundary conditions — Dirichlet, Neumann or mixed — retain their validity in this more general context. The corresponding self-adjoint boundary value problem takes the form

$$\nabla^* \circ \nabla u = -\,\frac{\partial}{\partial x}\left(p(x,y)\,\frac{\partial u}{\partial x} \right) - \frac{\partial}{\partial x}\left(q(x,y)\,\frac{\partial u}{\partial x} \right) = f(x,y), \qquad (x,y) \in \Omega, \tag{15.101}$$

along with the chosen boundary conditions.

The partial differential equation (15.101) arises in many other contexts. For example, consider a steady-state fluid flow described by a vector field $\mathbf{v}$ moving in a domain $\Omega \subset \mathbb{R}^2$. The flow is called *irrotational* if has zero curl, $\nabla \times \mathbf{v} = \mathbf{0}$, and hence, assuming Ω is simply connected, is a gradient $\mathbf{v} = \nabla u$. The function $u(x,y)$ is known as the fluid *velocity potential*. The constitutive assumptions connect the fluid velocity with its rate of flow $\mathbf{w} = \rho\,\mathbf{v}$, where $\rho(x,y) > 0$ is the scalar density of the fluid. Conservation of mass provides the final equation, namely $\nabla \cdot \mathbf{w} + f = 0$, where $f(x,y)$ represents fluid sources $f > 0$ or sinks $f < 0$. Therefore, the basic equilibrium equations take the form

$$-\nabla \cdot (\rho\, \nabla u) = f, \qquad \text{or} \qquad -\,\frac{\partial}{\partial x}\left(\rho(x,y)\,\frac{\partial u}{\partial x} \right) - \frac{\partial}{\partial y}\left(\rho(x,y)\,\frac{\partial u}{\partial y} \right) = f(x,y), \tag{15.102}$$

which is (15.101) with $p = q = \rho$. The most common case of a homogeneous (constant density) fluid thus reduces to the Poisson equation (15.3), with f replaced by f/ρ.

In electrostatics, the gradient equation $\mathbf{v} = \nabla u$ relates the voltage drop to the electrostatic potential u, and is the continuous analog of the circuit formula (6.18) relating potentials to voltages. The continuous version of Kirchhoff's Voltage Law (6.20) that the net voltage drop around any loop is zero is the fact that any gradient vector has zero curl, $\nabla \times \mathbf{v} = \mathbf{0}$, i.e., the flow is irrotational. Ohm's law (6.23) has the form $\mathbf{y} = C\,\mathbf{v}$ where the vector field $\mathbf{y}$ represents the current, while $C = \operatorname{diag}(p(x,y), q(x,y))$ represents th conductance of the medium; in the case of Laplace's equation, we are assuming a uniform unit conductance. Finally, the equation $f = \nabla \cdot \mathbf{y} = \nabla^* \mathbf{v}$ relating current and external current sources forms the continuous analog of Kirchhoff's Current Law (6.26) — the transpose of the discrete incidence matrix translates into the adjoint of the gradient operator is the divergence. Thus, our discrete electro-mechanical analogy carries over, in the continuous realm, to a tripartite electro-mechanical-fluid analogy, with all three physical systems leading to the exact same general mathematical structure.

Positive Definiteness and the Dirichlet Principle

In conclusion, as a result of the integration by parts calculation, we have formulated the Poisson and Laplace equations (as well as their weighted counterparts) in positive (semi-)definite, self-adjoint form

$$-\Delta u = \nabla^* \circ \nabla u = f,$$

when subject to the appropriate homogeneous boundary conditions: Dirichlet, Neumann, or mixed. A key benefit is, in the positive definite cases, the characterization of the solutions by a minimization principle.

According to Theorem 7.60, the self-adjoint operator $\nabla^* \circ \nabla$ is positive definite if and only if the kernel of the underlying gradient operator — restricted to the appropriate space of scalar fields — is trivial: $\ker \nabla = \{0\}$. The determination of the kernel of the gradient operator relies on the following elementary fact.

Lemma 15.13. *If $u(x,y)$ is a C^1 function defined on a connected domain Ω, then $\nabla u \equiv 0$ if and only if $u \equiv c$ is a constant.*

This result can be viewed as the multi-variable counterpart of the result that the only function with zero derivative is a constant. It is a simple consequence of Theorem A.20; see Exercise ■. Therefore, the only functions which could show up in $\ker \nabla$, and thus prevent positive definiteness, are the constants. The boundary conditions will tell us whether or not this occurs. The only constant function that satisfies either homogeneous Dirichlet or homogeneous mixed boundary conditions is the zero function, and thus, just as in the one-dimensional case, the boundary value problem for the Poisson equation with Dirichlet or mixed boundary conditions is positive definite. On the other hand, any constant function satisfies the homogeneous Neumann boundary conditions $\partial u/\partial \mathbf{n} = 0$, and hence such boundary value problems are only positive semi-definite.

In the positive definite cases, the equilibrium solution is characterized by our basic minimization principle (7.81). For the Poisson equation, the result is the justly famous *Dirichlet minimization principle*.

Theorem 15.14. *The function $u(x,y)$ that minimizes the* Dirichlet integral

$$\mathcal{P}[u] = \tfrac{1}{2} \| \nabla u \|^2 - \langle u\,; f \rangle = \iint_\Omega \left(\tfrac{1}{2} u_x^2 + \tfrac{1}{2} u_y^2 - f\,u \right) dx\,dy \tag{15.103}$$

among all C^1 functions that satisfy the prescribed homogeneous Dirichlet or mixed boundary conditions is the solution to the corresponding boundary value problem for the Poisson equation $-\Delta u = f$.

In physical applications, the Dirichlet integral (15.103) represents the energy in the system. As always, Nature chooses the equilibrium configuration so as to minimize the energy. A key application of the Dirichlet minimum principle is the finite element numerical solution scheme, to be described in detail in Section 15.5.

Remark: The fact that a minimizer to the Dirichlet integral (15.103) satisfies the Poisson equation is an immediate consequence of our general Minimization Theorem 7.62. However, unlike the finite-dimensional situation, proving the *existence* of a minimizing function is a non-trivial issue. This was not immediatiely recognized: Dirichlet originally thought this to be self-evident, but it then took about 50 years until Hilbert supplied the first rigorous existence proof. In this introductory treatment, we adopt a pragmatic approach, concentrating on the computation of the solution — reassured, if necessary, by the theoreticians' efforts in establishing its existence.

The Dirichlet minimization principle (15.103) was derived under the assumption that the boundary conditions are homogeneous — either pure Dirichlet or mixed. As it turns out, the principle, as stated, also applies to inhomogeneous Dirichlet boundary conditions. However, if we have a mixed boundary value problem with inhomogeneous Neumann conditions on part of the boundary, then we must include an additional boundary term in the minimizing functional. The general result can be stated as follows:

Theorem 15.15. *The solution $u(x,y)$ to the boundary value problem*

$$-\Delta u = f \quad \text{in} \quad \Omega, \qquad u = h \quad \text{on} \quad D, \qquad \frac{\partial u}{\partial \mathbf{n}} = k \quad \text{on} \quad N,$$

with $\partial\Omega = D \cup N$, and $D \neq \varnothing$, is characterized as the unique function that minimizes the modified Dirichlet integral

$$\widehat{\mathcal{P}}[u] = \iint_\Omega \left(\tfrac{1}{2} \| \nabla u \|^2 - f\,u \right) dx\,dy \;+\; \int_N u\,k\,ds \tag{15.104}$$

among all C^1 functions that satisfy the prescribed boundary conditions.

The inhomogeneous Dirichlet problem has $N = \varnothing$ and $D = \partial\Omega$, in which case the boundary integral does not appear. Exercise ■ asks you to prove this result.

As we know, positive definiteness is directly related to the stability of the physical system. The Dirichlet and mixed boundary value problems are stable, and can support any imposed force. On the other hand, the pure Neumann boundary value problem is unstable, owing to the existence of a nontrivial kernel — the constant functions. Physically,

the unstable mode represents a rigid translation of the entire membrane in the vertical direction. Indeed, the Neumann problem leaves the entire boundary of the membrane unattached to any support, and so the unforced membrane is free to move up or down without affecting its equilibrium status.

Furthermore, as in finite-dimensional linear systems, non-uniqueness and non-existence of solutions go hand in hand. As we learned in Section 11.3, the existence of a solution to a Neumann boundary value problem is subject to the *Fredholm alternative*, suitably adapted to this multi-dimensional situation. A necessary condition for the existence of a solution is that the forcing function be orthogonal to the elements of the kernel of the underlying self-adjoint linear operator, which, in the present situation requires that f be orthogonal to the subspace consisting of all constant functions. In practical terms, we only need to check orthogonality with respect to a basis for the subspace, which in this situation consists of the constant function 1.

Theorem 15.16. *The Neumann boundary value problem*

$$-\Delta u = f, \quad \text{in} \quad \Omega, \qquad\qquad \frac{\partial u}{\partial \mathbf{n}} = 0, \quad \text{on} \quad \partial\Omega, \tag{15.105}$$

admits a solution $u(x,y)$ if and only if

$$\langle\, 1\,;\, f\,\rangle = \iint_\Omega f(x,y)\,dx\,dy = 0. \tag{15.106}$$

Moreover, when it exists, the solution is not unique since any function of the form $u(x,y)+c$, where $c \in \mathbb{R}$ is an arbitrary constant, is also a solution.

Forcing functions $f(x,y)$ which do not satisfy the orthogonality constraint (15.106) will excite the translational instability, and no equilibrium configuration is possible. For example, if we force a free membrane, (15.106) requires that the net force in the vertical direction be zero; otherwise, the membrane will start moving and cannot be in an equilibrium.

15.5. Finite Elements.

As the reader has no doubt already surmised, explicit solutions to boundary value problems for the Laplace and Poisson equations are few and far between. In most cases, exact solution formulae are not available, or are so complicated as to be of scant utility. To proceed further, one is forced to design suitable numerical approximation schemes that can accurately evaluate the desired solution.

An especially powerful class of numerical algorithms for solving elliptic boundary value problems are the finite element methods. We have already learned, in Section 11.6, the key underlying idea. One begins with a minimization principle, prescribed by a quadratic functional defined on a suitable vector space of functions U that serves to incorporate the (homogeneous) boundary conditions. The desired solution is characterized as the unique minimizer $u_\star \in U$. One then restricts the functional to a suitably chosen finite-dimensional subspace $W \subset U$, and seeks a minimizer $w_\star \in W$. Finite-dimensionality of

W has the effect of reducing the infinite-dimensional minimization problem to a finite-dimensional problem, which can then be solved by numerical linear algebra. The resulting minimizer $w_\star$ will — provided the subspace W has been cleverly chosen — provide a good approximation to the true minimizer $u_\star$ on the entire domain. Here we concentrate on the practical design of the finite element procedure, and refer the reader to a more advanced text, e.g., [**174**], for the analytical details and proofs of convergence. Most of the multi-dimensional complications are not in the underlying theory, but rather in the realms of data management and organizational details.

In this section, we first concentrate on applying these ideas to the two-dimensional Poisson equation. For specificity, we concentrate on the homogeneous Dirichlet boundary value problem

$$-\Delta u = f \quad \text{in} \quad \Omega \qquad\qquad u = 0 \quad \text{on} \quad \partial\Omega. \tag{15.107}$$

According to Theorem 15.14, the solution $u = u_\star$ is characterized as the unique minimizing function for the Dirichlet functional (15.103) among all smooth functions $u(x, y)$ that satisfy the prescribed boundary conditions. In the finite element approximation, we restrict the Dirichlet functional to a suitably chosen finite-dimensional subspace. As in the one-dimensional situation, the most convenient finite-dimensional subspaces consist of functions that may lack the requisite degree of smoothness that qualifies them as possible solutions to the partial differential equation. Nevertheless, they do provide good approximations to the actual solution. An important practical consideration, impacting the speed of the calculation, is to employ functions with small support, as in Definition 13.5. The resulting finite element matrix will then be sparse and the solution to the linear system can be relatively rapidly calculate, usually by application of an iterative numerical scheme such as the Gauss–Seidel or SOR methods discussed in Chapter 10.

Finite Elements and Triangulation

For one-dimensional boundary value problems, the finite element construction rests on the introduction of a mesh $a = x_0 < x_1 < \cdots < x_n = b$ on the interval of definition. The mesh nodes x_k break the interval into a collection of small subintervals. In two-dimensional problems, a *mesh* consists of a finite number of points $\mathbf{x}_k = (x_k, y_k)$, $k = 1, \ldots, m$, known as *nodes*, usually lying inside the domain $\Omega \subset \mathbb{R}^2$. As such, there is considerable freedom in the choice of mesh nodes, and completely uniform spacing is often not possible. We regard the nodes as forming the vertices of a *triangulation* of the domain Ω, consisting of a finite number of small triangles, which we denote by $T_1, \ldots, T_N$. The nodes are split into two categories — *interior nodes* and *boundary nodes*, the latter lying on or close to the boundary of the domain. A curved boundary is approximated by the polygon through the boundary nodes formed by the sides of the triangles lying on the edge of the domain; see Figure 15.10 for a typical example. Thus, in computer implementations of the finite element method, the first module is a routine that will automatically triangulate a specified domain in some reasonable manner; see below for details on what "reasonable" entails.

As in our one-dimensional finite element construction, the functions $w(x, y)$ in the finite-dimensional subspace W will be continuous and *piecewise affine*. "Piecewise affine"

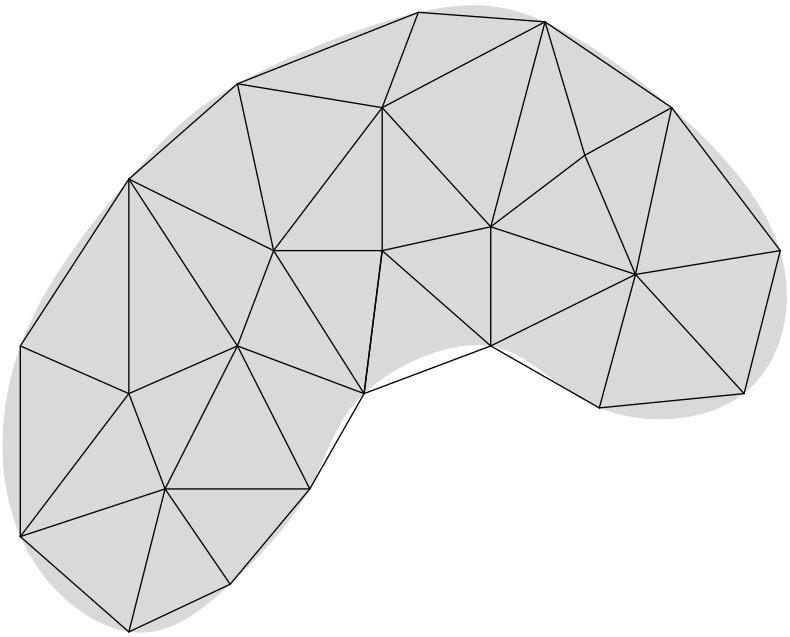

Figure 15.10. Triangulation of a Planar Domain.

means that, on each triangle, the graph of w is flat, and so has the formula[†]

$$w(x,y) = \alpha^\nu + \beta^\nu\, x + \gamma^\nu\, y, \qquad \text{for} \qquad (x,y) \in T_\nu. \tag{15.108}$$

Continuity of w requires that its values on a common edge between two triangles must agree, and this will impose certain compatibility conditions on the coefficients $\alpha^\mu, \beta^\mu, \gamma^\mu$ and $\alpha^\nu, \beta^\nu, \gamma^\nu$ associated with adjacent pairs of triangles T_μ, T_ν. The graph of $z = w(x,y)$ forms a connected polyhedral surface whose triangular faces lie above the triangles in the domain; see Figure 15.10 for an illustration.

The next step is to choose a basis of the subspace of piecewise affine functions for the given triangulation. As in the one-dimensional version, the most convenient basis consists of *pyramid functions* $\varphi_k(x,y)$ which assume the value 1 at a single node $\mathbf{x}_k$, and are zero at all the other nodes; thus

$$\varphi_k(x_i, y_i) = \begin{cases} 1, & i = k, \\ 0, & i \neq k. \end{cases} \tag{15.109}$$

Note that φ_k will be nonzero only on those triangles which have the node $\mathbf{x}_k$ as one of their vertices, and hence the graph of φ_k looks like a pyramid of unit height sitting on a flat plane, as illustrated in Figure 15.12.

The pyramid functions $\varphi_k(x,y)$ corresponding to the *interior nodes* $\mathbf{x}_k$ automatically satisfy the homogeneous Dirichlet boundary conditions on the boundary of the domain — or, more correctly, on the polygonal boundary of the triangulated domain, which is

[†] Here and subsequently, the index ν is a superscript, not a power!

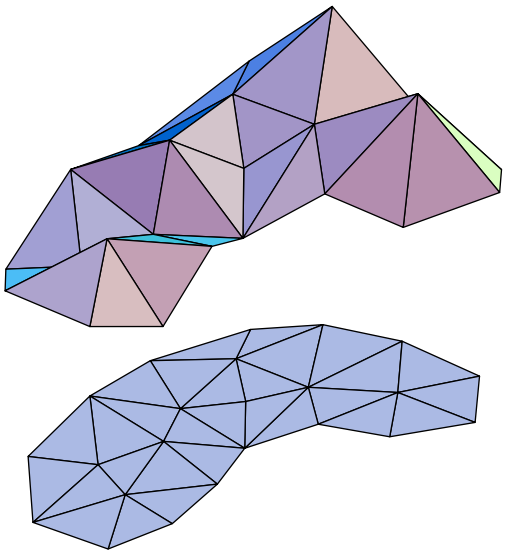

Figure 15.11. Piecewise Affine Function.

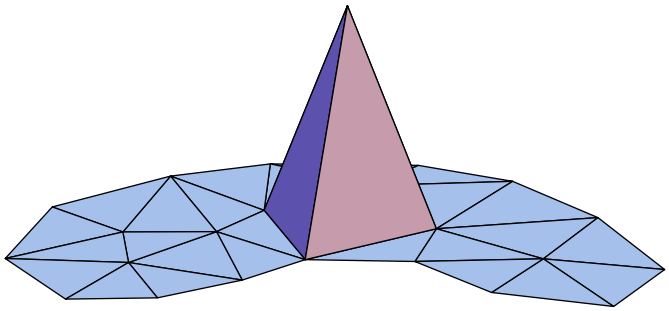

Figure 15.12. Finite Element Pyramid Function.

supposed to be a good approximation to the curved boundary of the original domain Ω. Thus, the finite-dimensional finite element subspace W is the span of the interior node pyramid functions, and so general element $w \in W$ is a linear combination thereof:

$$w(x,y) = \sum_{k=1}^{n} c_k \, \varphi_k(x,y), \tag{15.110}$$

where the sum ranges over the n interior nodes of the triangulation. Owing to the original specification (15.109) of the pyramid functions, the coefficients

$$c_k = w(x_k, y_k) \approx u(x_k, y_k), \qquad k = 1, \dots, n, \tag{15.111}$$

are the *same* as the values of the finite element approximation $w(x,y)$ at the interior

nodes. This immediately implies linear independence of the pyramid functions, since the only linear combination that vanishes at all nodes is the trivial one $c_1 = \cdots = c_n = 0$. Thus, the interior node pyramid functions $\varphi_1, \dots \varphi_n$ form a basis for finite element subspace W, which therefore has dimension equal to n, the number of interior nodes.

Determining the explicit formulae for the finite element basis functions is not difficult. On one of the triangles T_ν that has $\mathbf{x}_k$ as a vertex, $\varphi_k(x,y)$ will be the unique affine function (15.108) that takes the value 1 at the vertex $\mathbf{x}_k$ and 0 at its other two vertices $\mathbf{x}_l$ and $\mathbf{x}_m$. Thus, we are in need of a formula for an affine function or *element*

$$\omega_k^\nu(x,y) = \alpha_k^\nu + \beta_k^\nu\, x + \gamma_k^\nu\, y, \qquad\qquad (x,y) \in T_\nu, \tag{15.112}$$

that takes the prescribed values

$$\omega_k^\nu(x_i,y_i) = \omega_k^\nu(x_j,y_j) = 0, \qquad\qquad \omega_k^\nu(x_k,y_k) = 1,$$

at three distinct points. These three conditions lead to the linear system

$$\begin{aligned} \omega_k^\nu(x_i,y_i) &= \alpha_k^\nu + \beta_k^\nu\, x_i + \gamma_k^\nu\, y_i \;= 0,\\ \omega_k^\nu(x_j,y_j) &= \alpha_k^\nu + \beta_k^\nu\, x_j + \gamma_k^\nu\, y_j \;= 0,\\ \omega_k^\nu(x_k,y_k) &= \alpha_k^\nu + \beta_k^\nu\, x_k + \gamma_k^\nu\, y_k = 1. \end{aligned} \tag{15.113}$$

The solution[†] produces the explicit formulae

$$\alpha_k^\nu = \frac{x_i\, y_j - x_j\, y_i}{\Delta_\nu}\,, \qquad\qquad \beta_k^\nu = \frac{y_i - y_j}{\Delta_\nu}\,, \qquad\qquad \gamma_k^\nu = \frac{x_j - x_i}{\Delta_\nu}\,, \tag{15.114}$$

for the coefficients; the denominator

$$\Delta_\nu = \det \begin{pmatrix} 1 & x_i & y_i \\ 1 & x_j & y_j \\ 1 & x_k & y_k \end{pmatrix} = \pm 2 \,\text{area}\, T_\nu \tag{15.115}$$

is, up to sign, twice the area of the triangle T_ν; see Exercise ■.

Example 15.17. Consider an isoceles right triangle T with vertices

$$\mathbf{x}_1 = (0,0), \qquad\qquad \mathbf{x}_2 = (1,0), \qquad\qquad \mathbf{x}_3 = (0,1).$$

Using (15.114–115) (or solving the linear systems (15.113) directly), we immediately produce the three affine elements

$$\omega_1(x,y) = 1 - x - y, \qquad\qquad \omega_2(x,y) = x, \qquad\qquad \omega_3(x,y) = y. \tag{15.116}$$

As required, each ω_k equals 1 at the vertex $\mathbf{x}_k$ and is zero at the other two vertices.

[†] Cramer's Rule (1.88) comes in handy here.

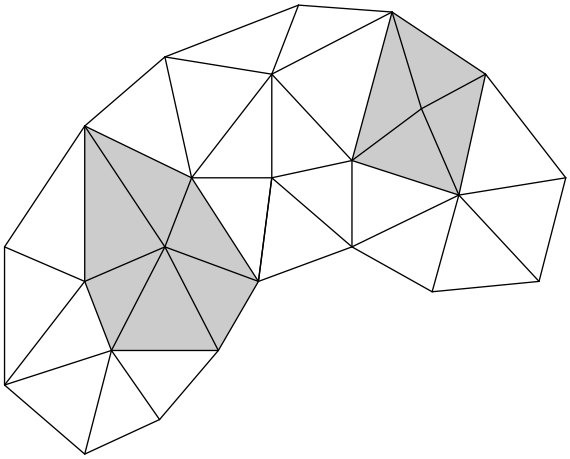

Figure 15.13. Vertex Polygons.

The finite element pyramid function is then obtained by piecing together the individual affine elements, whence

$$\varphi_k(x,y) = \begin{cases} \omega_k^{\nu}(x,y), & \text{if } (x,y) \in T_{\nu} \text{ which has } \mathbf{x}_k \text{ as a vertex,} \\ 0, & \text{otherwise.} \end{cases} \tag{15.117}$$

Continuity of $\varphi_k(x,y)$ is assured since the constituent affine elements have the same values at common vertices. The support of the pyramid function (15.117) is the polygon

$$\operatorname{supp} \varphi_k = P_k = \bigcup_{\nu} T_{\nu} \tag{15.118}$$

consisting of all the triangles T_{ν} that have the node $\mathbf{x}_k$ as a vertex. In other words, $\varphi_k(x,y) = 0$ whenever $(x,y) \notin P_k$. We will call P_k the k^{th} *vertex polygon*. The node $\mathbf{x}_k$ lies on the interior of its vertex polygon P_k, while the vertices of P_k are all those that are connected to $\mathbf{x}_k$ by a single edge of the triangulation. In Figure 15.13 the shaded regions indicate two of the vertex polygons for the triangulation in Figure 15.10.

Example 15.18. The simplest, and most common triangulations are based on regular meshes. Suppose that the nodes lie on a square grid, and so are of the form $\mathbf{x}_{i,j} = (i\,h + a, j\,h + b)$ where $h > 0$ is the inter-node spacing, and (a,b) represents an overall offset. If we choose the triangles to all have the same orientation, as in the first picture in Figure 15.14, then the vertex polygons all have the same shape, consisting of 6 triangles of total area $3h^2$ — the shaded region. On the other hand, if we choose an alternating, perhaps more æsthetically pleasing triangulation as in the second picture, then there are two types of vertex polygons. The first, consisting of four triangles, has area $2h^2$, while the second, containing 8 triangles, has twice the area, $4h^2$. In practice, there are good reasons to prefer the former triangulation.

In general, in order to ensure convergence of the finite element solution to the true minimizer, one should choose a triangulation with the following properties:

(*a*) The triangles are not too long and skinny. In other words, their sides should have comparable lengths. In particular, obtuse triangles should be avoided.

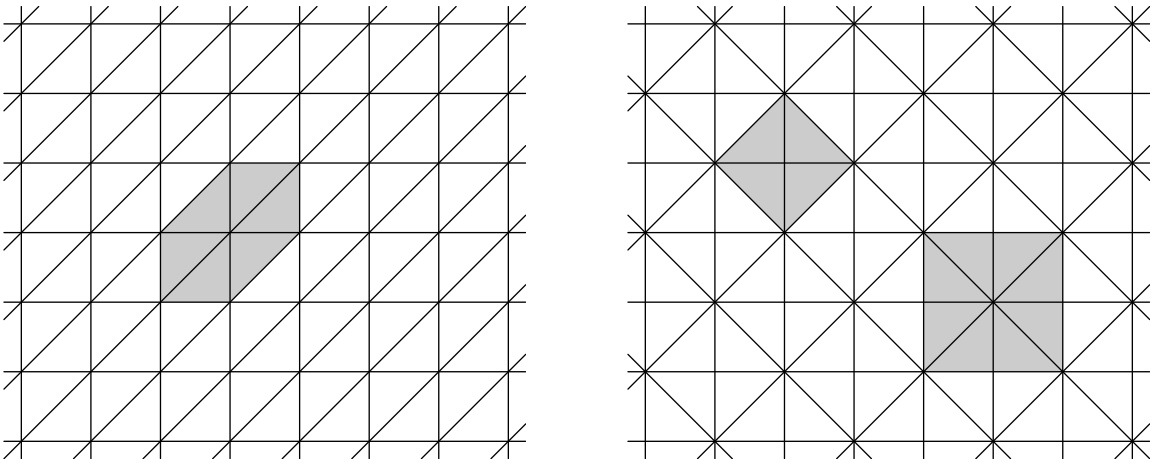

Figure 15.14. Square Mesh Triangulations.

(*b*) The areas of nearby triangles T_ν should not vary too much.

(*c*) The areas of nearby vertex polygons P_k should also not vary too much.

For adaptive or variable meshes, one might very well have wide variations in area over the entire grid, with small triangles in regions of rapid change in the solution, and large ones in less interesting regions. But, overall, the sizes of the triangles and vertex polygons should not dramatically vary as one moves across the domain.

The Finite Element Equations

We now seek to approximate the solution to the homogeneous Dirichlet boundary value problem by restricting the Dirichlet functional to the selected finite element subspace W. Substituting the formula (15.110) for a general element of W into the quadratic Dirichlet functional (15.103) and expanding, we find

$$\begin{aligned} \mathcal{P}[w] = \mathcal{P}\left[\sum_{i=1}^{n} c_i\,\varphi_i\right] &= \iint_\Omega \left[\left(\sum_{i=1}^{n} c_i\,\nabla\varphi_i\right)^2 - f(x,y)\left(\sum_{i=1}^{n} c_i\,\varphi_i\right)\right] dx\,dy \\ &= \frac{1}{2}\sum_{i,j=1}^{n} k_{ij}\,c_i\,c_j - \sum_{i=1}^{n} b_i\,c_i = \tfrac{1}{2}\,\mathbf{c}^T K\,\mathbf{c} - \mathbf{b}^T\mathbf{c}. \end{aligned}$$

Here, $K = (k_{ij})$ is the symmetric $n \times n$ matrix, while $\mathbf{b} = (\,b_1, b_2, \ldots, b_n\,)^T$ is the vector that have the respective entries

$$\begin{aligned} k_{ij} &= \langle\,\nabla\varphi_i\,;\nabla\varphi_j\,\rangle = \iint_\Omega \nabla\varphi_i\cdot\nabla\varphi_j\,dx\,dy, \\ b_i &= \langle\,f\,;\varphi_i\,\rangle = \iint_\Omega f\,\varphi_i\,dx\,dy. \end{aligned} \tag{15.119}$$

Thus, to determine the finite element approximation, we need to minimize the quadratic function

$$P(\mathbf{c}) = \tfrac{1}{2}\,\mathbf{c}^T K\,\mathbf{c} - \mathbf{b}^T\mathbf{c} \tag{15.120}$$

over all possible choices of coefficients $\mathbf{c} = (\,c_1, c_2, \ldots, c_n\,)^T \in \mathbb{R}^n$, i.e., over all possible function values at the interior nodes. Restricting to the finite element subspace has reduced us to a standard finite-dimensional quadratic minimization problem. First, the coefficient matrix $K > 0$ is positive definite due to the positive definiteness of the original functional; the proof in Section 11.6 is easily adapted to the present situation. Theorem 4.1 tells us that the minimizer is obtained by solving the associated linear system

$$K\,\mathbf{c} = \mathbf{b}. \tag{15.121}$$

The solution to (15.121) can be effected by either Gaussian elimination or an iterative technique.

To find explicit formulae for the matrix coefficients k_{ij} in (15.119), we begin by noting that the gradient of the affine element (15.112) is equal to

$$\nabla \omega_k^\nu(x,y) = \mathbf{a}_k^\nu = \begin{pmatrix} \beta_k^\nu \\ \gamma_k^\nu \end{pmatrix} = \frac{1}{\Delta_\nu}\begin{pmatrix} y_i - y_j \\ x_j - x_i \end{pmatrix}, \qquad (x,y) \in T_\nu, \tag{15.122}$$

which is a constant vector inside the triangle T_ν, while outside $\nabla \omega_k^\nu = \mathbf{0}$. Therefore,

$$\nabla \varphi_k(x,y) = \begin{cases} \nabla \omega_k^\nu = \mathbf{a}_k^\nu, & \text{if } (x,y) \in T_\nu \text{ which has } \mathbf{x}_k \text{ as a vertex,} \\ \mathbf{0}, & \text{otherwise,} \end{cases} \tag{15.123}$$

reduces to a piecewise constant function on the triangulation. Actually, (15.123) is not quite correct since if (x,y) lies on the boundary of a triangle T_ν, then the gradient does not exist. However, this technicality will not cause any difficulty in evaluating the ensuing integral.

We will approximate integrals over the domain Ω by integrals over the triangles, which relies on our assumption that the polygonal boundary of the triangulation is a reasonably close approximation to the true boundary $\partial\Omega$. In particular,

$$k_{ij} \;\approx\; \sum_\nu \iint_{T_\nu} \nabla \varphi_i \cdot \nabla \varphi_j \, dx\, dy \;\equiv\; \sum_\nu k_{ij}^\nu. \tag{15.124}$$

Now, according to (15.123), one or the other gradient in the integrand will vanish on the entire triangle T_ν *unless* both $\mathbf{x}_i$ and $\mathbf{x}_j$ are vertices. Therefore, the only terms contributing to the sum are those triangles T_ν that have both $\mathbf{x}_i$ and $\mathbf{x}_j$ as vertices. If $i \neq j$ there are only two such triangles, while if $i = j$ every triangle in the i^{th} vertex polygon P_i contributes. The individual summands are easily evaluated, since the gradients are constant on the triangles, and so, by (15.123),

$$k_{ij}^\nu = \iint_{T_\nu} \mathbf{a}_i^\nu \cdot \mathbf{a}_j^\nu \; dx\, dy = \mathbf{a}_i^\nu \cdot \mathbf{a}_j^\nu \text{ area } T_\nu = \tfrac{1}{2}\,\mathbf{a}_i^\nu \cdot \mathbf{a}_j^\nu \;|\,\Delta_\nu\,|\,.$$

Figure 15.15. Right and Equilateral Triangles.

Let T_ν have vertices $\mathbf{x}_i, \mathbf{x}_j, \mathbf{x}_k$. Then, by (15.122, 123, 115),

$$k_{ij}^\nu = \frac{1}{2}\,\frac{(y_j - y_k)(y_k - y_i) + (x_k - x_j)(x_i - x_k)}{(\Delta_\nu)^2}\,|\,\Delta_\nu\,| = -\,\frac{(\mathbf{x}_i - \mathbf{x}_k)\cdot(\mathbf{x}_j - \mathbf{x}_k)}{2\,|\,\Delta_\nu\,|}\,, \quad i \neq j,$$
$$k_{ii}^\nu = \frac{1}{2}\,\frac{(y_j - y_k)^2 + (x_k - x_j)^2}{(\Delta_\nu)^2}\,|\,\Delta_\nu\,| = \frac{\|\,\mathbf{x}_j - \mathbf{x}_k\,\|^2}{2\,|\,\Delta_\nu\,|}\,. \tag{15.125}$$

In this manner, each triangle T_ν specifies a collection of 6 different coefficients, $k_{ij}^\nu = k_{ji}^\nu$, indexed by its vertices, and known as the *elemental stiffnesses* of T_ν. Interestingly, the elemental stiffnesses depend only on the three vertex *angles* in the triangle and not on its size. Thus, similar triangles have the *same* elemental stiffnesses. Indeed, if $\theta_i^\nu, \theta_j^\nu, \theta_k^\nu$ denote the angles in T_ν at the respective vertices $\mathbf{x}_i, \mathbf{x}_j, \mathbf{x}_k$, then, according to Exercise ■,

$$k_{ii}^\nu = \tfrac{1}{2}\big(\cot\theta_k^\nu + \cot\theta_j^\nu\big), \qquad \text{while} \qquad k_{ij}^\nu = k_{ji}^\nu = -\tfrac{1}{2}\cot\theta_k^\nu, \quad i \neq j. \tag{15.126}$$

Example 15.19. The right triangle with vertices $\mathbf{x}_1 = (0,0)$, $\mathbf{x}_2 = (1,0)$, $\mathbf{x}_3 = (0,1)$ has elemental stiffnesses

$$k_{11} = 1, \qquad k_{22} = k_{33} = \tfrac{1}{2}, \qquad k_{12} = k_{21} = k_{13} = k_{31} = -\tfrac{1}{2}, \qquad k_{23} = k_{32} = 0. \tag{15.127}$$

The same holds for any other isoceles right triangle, as long as we chose the first vertex to be at the right angle. Similarly, an equilateral triangle has all 60° angles, and so its elemental stiffnesses are

$$\begin{aligned} &k_{11} = k_{22} = k_{33} = \tfrac{1}{\sqrt{3}} \approx .577350, \\ &k_{12} = k_{21} = k_{13} = k_{31} = k_{23} = k_{32} = -\tfrac{1}{2\sqrt{3}} \approx -.288675. \end{aligned} \tag{15.128}$$

Assembling the Elements

The elemental stiffnesses of each triangle will contribute, through the summation (15.124), to the finite element coefficient matrix K. We begin by constructing a larger matrix K^*, which we call the *full finite element matrix*, of size $m \times m$ where m is the total number of nodes in our triangulation, including both interior and boundary nodes. The rows and columns of K^* are labeled by the nodes $\mathbf{x}_i$. Let $K_\nu = (k_{ij}^\nu)$ be the corresponding $m \times m$ matrix containing the elemental stiffnesses k_{ij}^ν of T_ν in the rows and columns indexed

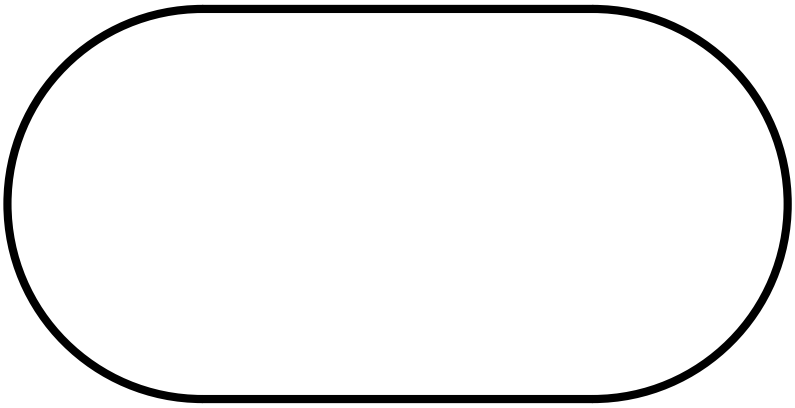

Figure 15.16. The Oval Plate.

by its vertices, and all other entries equal to 0. Thus, K_ν will have (at most) 9 nonzero entries. The resulting $m \times m$ matrices are all summed together over all the triangles,

$$K^* = \sum_{\nu=1}^{N} K_\nu, \tag{15.129}$$

to produce the full finite element matrix, in accordance with (15.124).

The full finite element matrix K^* is too large, since its rows and columns include all the nodes, whereas the finite element matrix K appearing in (15.121) only refers to the n interior nodes. The *reduced* $n \times n$ *finite element matrix* K is simply obtained from K^* by deleting all rows and columns indexed by boundary nodes, retaining only the elements k_{ij} when both $\mathbf{x}_i$ and $\mathbf{x}_j$ are interior nodes. (This may remind the reader of our construction of the reduced incidence matrix for a structure in Chapter 6.) For the homogeneous boundary value problem, this is all we require. As we shall see, inhomogeneous boundary conditions are most easily handled by retaining (part of) the full matrix K^*.

The easiest way to digest the construction is by working through a particular example.

Example 15.20. A metal plate has the shape of an oval running track, consisting of a rectangle, with side lengths 1 m by 2 m, and two semicircular disks glued onto its shorter ends, as sketched in Figure 15.16. The plate is subject to a heat source while its edges are held at a fixed temperature. The problem is to find the equilibrium temperature distribution within the plate. Mathematically, we must solve the Poisson equation with Dirichlet boundary conditions, for the equilibrium temperature $u(x, y)$.

Let us describe how to set up the finite element approximation to such a boundary value problem. We begin with a very coarse triangulation of the plate, which will not give particularly accurate results, but does serve to illustrate how to go about assembling the finite element matrix. We divide the rectangular part of the plate into 8 right triangles, while each semicircular end will be approximated by three equilateral triangles. The triangles are numbered from 1 to 14 as indicated in Figure 15.17. There are 13 nodes in all, numbered as in the second figure. Only nodes $1, 2, 3$ are interior, while the boundary nodes are labeled 4 through 13, going counterclockwise around the boundary starting at the top.

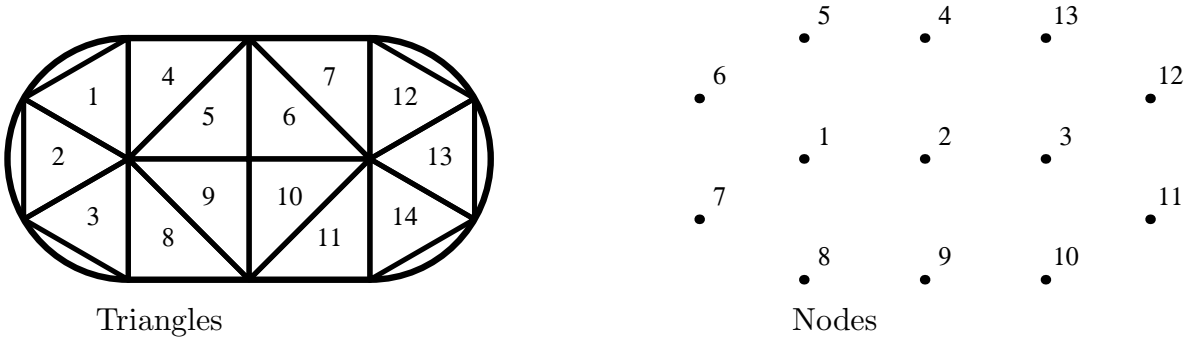

Figure 15.17. A Coarse Triangulation of the Oval Plate.

The full finite element matrix K^* will have size 13×13, its rows and columns labeled by all the nodes, while the reduced matrix K appearing in the finite element equations (15.121) consists of the upper left 3×3 submatrix of K^* corresponding to the three interior nodes.

Each triangle T_ν will contribute the summand K_ν whose values are its elemental stiffnesses, as indexed by its vertices. For example, the first triangle T_1 is equilateral, and so has elemental stiffnesses (15.128). Its vertices are labeled 1, 5, and 6, and therefore we place the stiffnesses (15.128) in the rows and columns numbered $1, 5, 6$ to form the summand

$$K_1 = \begin{pmatrix} .577350 & 0 & 0 & 0 & -.288675 & -.288675 & 0 & 0 & \dots \\ 0 & 0 & 0 & 0 & 0 & 0 & 0 & 0 & \dots \\ 0 & 0 & 0 & 0 & 0 & 0 & 0 & 0 & \dots \\ 0 & 0 & 0 & 0 & 0 & 0 & 0 & 0 & \dots \\ -.288675 & 0 & 0 & 0 & .577350 & -.288675 & 0 & 0 & \dots \\ -.288675 & 0 & 0 & 0 & -.288675 & .577350 & 0 & 0 & \dots \\ 0 & 0 & 0 & 0 & 0 & 0 & 0 & 0 & \dots \\ 0 & 0 & 0 & 0 & 0 & 0 & 0 & 0 & \dots \\ \vdots & \vdots & \vdots & \vdots & \vdots & \vdots & \vdots & \vdots & \ddots \end{pmatrix},$$

where all the undisplayed entries in the full 13×13 matrix are 0. The next triangle T_2 has the same equilateral elemental stiffness matrix (15.128), but now its vertices are $1, 6, 7$, and so it will contribute

$$K_2 = \begin{pmatrix} .577350 & 0 & 0 & 0 & 0 & -.288675 & -.288675 & 0 & \dots \\ 0 & 0 & 0 & 0 & 0 & 0 & 0 & 0 & \dots \\ 0 & 0 & 0 & 0 & 0 & 0 & 0 & 0 & \dots \\ 0 & 0 & 0 & 0 & 0 & 0 & 0 & 0 & \dots \\ 0 & 0 & 0 & 0 & 0 & 0 & 0 & 0 & \dots \\ -.288675 & 0 & 0 & 0 & 0 & .577350 & -.2886750 & 0 & \dots \\ -.288675 & 0 & 0 & 0 & 0 & -.288675 & .5773500 & 0 & \dots \\ 0 & 0 & 0 & 0 & 0 & 0 & 0 & 0 & \dots \\ \vdots & \vdots & \vdots & \vdots & \vdots & \vdots & \vdots & \vdots & \ddots \end{pmatrix}.$$

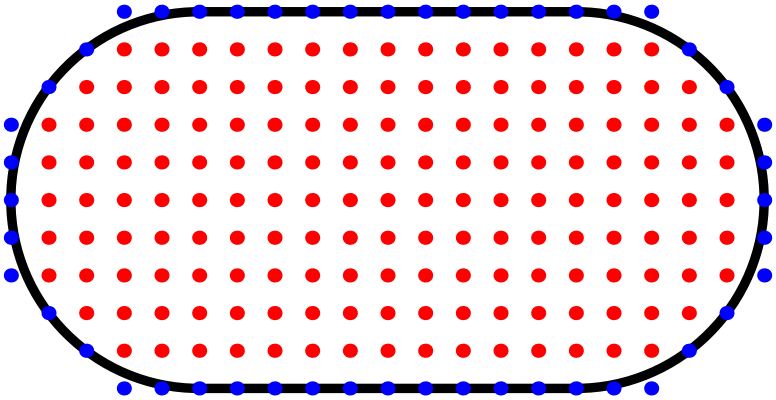

Figure 15.18. A Square Mesh for the Oval Plate.

Similarly for K_3, with vertices $1, 7, 8$. On the other hand, triangle T_4 is an isoceles right triangle, and so has elemental stiffnesses (15.127). Its vertices are labeled 1, 4, and 5, with vertex 5 at the right angle. Therefore, its contribution is

$$K_4 = \begin{pmatrix} .5 & 0 & 0 & 0 & -.5 & 0 & 0 & 0 & \dots \\ 0 & 0 & 0 & 0 & 0 & 0 & 0 & 0 & \dots \\ 0 & 0 & 0 & 0 & 0 & 0 & 0 & 0 & \dots \\ 0 & 0 & 0 & .5 & -.5 & 0 & 0 & 0 & \dots \\ -.5 & 0 & 0 & -.5 & 1.0 & 0 & 0 & 0 & \dots \\ 0 & 0 & 0 & 0 & 0 & 0 & 0 & 0 & \dots \\ 0 & 0 & 0 & 0 & 0 & 0 & 0 & 0 & \dots \\ 0 & 0 & 0 & 0 & 0 & 0 & 0 & 0 & \dots \\ \vdots & \vdots & \vdots & \vdots & \vdots & \vdots & \vdots & \vdots & \ddots \end{pmatrix}.$$

Continuing in this manner, we assemble 14 contributions $K_1, \dots, K_{14}$, each with (at most) 9 nonzero entries. The full finite element matrix is the sum

$$\begin{aligned} K^* &= K_1 + K_2 + \cdots + K_{14} \\ &= \begin{pmatrix} 3.732 & -1 & 0 & 0 & -.7887 & -.5774 & -.5774 \\ -1 & 4 & -1 & -1 & 0 & 0 & 0 \\ 0 & -1 & 3.732 & 0 & 0 & 0 & 0 \\ 0 & -1 & 0 & 2 & -.5 & 0 & 0 \\ -.7887 & 0 & 0 & -.5 & 1.577 & -.2887 & 0 \\ -.5774 & 0 & 0 & 0 & -.2887 & 1.155 & -.2887 \\ -.5774 & 0 & 0 & 0 & 0 & -.2887 & 1.155 \\ -.7887 & 0 & 0 & 0 & 0 & 0 & -.2887 \\ 0 & -1 & 0 & 0 & 0 & 0 & 0 \\ 0 & 0 & -.7887 & 0 & 0 & 0 & 0 \\ 0 & 0 & -.5774 & 0 & 0 & 0 & 0 \\ 0 & 0 & -.5774 & 0 & 0 & 0 & 0 \\ 0 & 0 & -.7887 & -.5 & 0 & 0 & 0 \end{pmatrix} \end{aligned} \tag{15.130}$$

$$\begin{pmatrix} -.7887 & 0 & 0 & 0 & 0 & 0 \\ 0 & -1 & 0 & 0 & 0 & 0 \\ 0 & 0 & -.7887 & -.5774 & -.5774 & -.7887 \\ 0 & 0 & 0 & 0 & 0 & -.5 \\ 0 & 0 & 0 & 0 & 0 & 0 \\ 0 & 0 & 0 & 0 & 0 & 0 \\ -.2887 & 0 & 0 & 0 & 0 & 0 \\ 1.577 & -.5 & 0 & 0 & 0 & 0 \\ -.5 & 2 & -.5 & 0 & 0 & 0 \\ 0 & -.5 & 1.577 & -.2887 & 0 & 0 \\ 0 & 0 & -.2887 & 1.155 & -.2887 & 0 \\ 0 & 0 & 0 & -.2887 & 1.155 & -.2887 \\ 0 & 0 & 0 & 0 & -.2887 & 1.577 \end{pmatrix}.$$

Since only nodes $1, 2, 3$ are interior nodes, the reduced finite element matrix only uses the upper left 3×3 block of K^*, so

$$K = \begin{pmatrix} 3.732 & -1 & 0 \\ -1 & 4 & -1 \\ 0 & -1 & 3.732 \end{pmatrix}. \tag{15.131}$$

It is not difficult to directly construct K, bypassing K^* entirely.

For a finer triangulation, the construction is similar, but the matrices become much larger. The procedure can, of course, be automated. Fortunately, if we choose a very regular triangulation, then we do not need to be nearly as meticulous in assembling the stiffness matrices, since many of the entries are the same. The simplest case is when we use a uniform square mesh, and so triangulate the domain into isoceles right triangles. This is accomplished by laying out a relatively dense square grid over the domain $\Omega \subset \mathbb{R}^2$. The interior nodes are the grid points that fall inside the oval domain, while the boundary nodes are all those grid points lying adjacent to one or more of the interior nodes, and are near but not necessarily precisely on the boundary $\partial\Omega$. Figure 15.18 shows the nodes in a square grid with intermesh spacing $h = .2$. While a bit crude in its approximation of the boundary of the domain, this procedure does have the advantage of making the construction of the associated finite element matrix relatively painless.

For such a mesh, all the triangles are isoceles right triangles, with elemental stiffnesses (15.127). Summing the corresponding matrices K_ν over all the triangles, as in (15.129), the rows and columns of K^* corresponding to the interior nodes are seen to all have the same form. Namely, if i labels an interior node, then the corresponding diagonal entry is $k_{ii} = 4$, while the off-diagonal entries $k_{ij} = k_{ji}$, $i \neq j$, are equal to either -1 when node i is adjacent to node j on the grid, and is equal to 0 in all other cases. Node j is allowed to be a boundary node. (Interestingly, the result does not depend on how one orients the pair of triangles making up each square of the grid, which only plays a role in the computation of the right hand side of the finite element equation.) Observe that the same computation applies even to our coarse triangulation. The interior node 2 belongs to all right isoceles triangles, and the corresponding entries in (15.130) are $k_{22} = 4$, and $k_{2j} = -1$ for the four adjacent nodes $j = 1, 3, 4, 9$.

Remark: Interestingly, the coefficient matrix arising from the finite element method on a square (or even rectangular) grid is the same as the coefficient matrix arising from a

finite difference solution to the Laplace or Poisson equation, as described in Exercise ■. The finite element approach has the advantage of applying to much more general triangulations.

In general, while the finite element matrix K for a two-dimensional boundary value problem is not as nice as the tridiagonal matrices we obtained in our one-dimensional problems, it is still very sparse and, on regular grids, highly structured. This makes solution of the resulting linear system particularly amenable to an iterative matrix solver such as Gauss–Seidel, Jacobi, or, for even faster convergence, successive over-relaxation (SOR).

The Coefficient Vector and the Boundary Conditions

So far, we have been concentrating on assembling the finite element coefficient matrix K. We also need to compute the forcing vector $\mathbf{b} = (\, b_1, b_2, \dots, b_n \,)^T$ appearing on the right hand side of the fundamental linear equation (15.121). According to (15.119), the entries b_i are found by integrating the product of the forcing function and the finite element basis function. As before, we will approximate the integral over the domain Ω by an integral over the triangles, and so

$$b_i = \iint_\Omega f\, \varphi_i \, dx\, dy \approx \sum_\nu \iint_{T_\nu} f\, \omega_i^\nu \, dx\, dy \equiv \sum_\nu b_i^\nu. \tag{15.132}$$

Typically, the exact computation of the various triangular integrals is not convenient, and so we resort to a numerical approximation. Since we are assuming that the individual triangles are small, we can adopt a very crude numerical integration scheme. If the function $f(x, y)$ does not vary much over the triangle T_ν — which will certainly be the case if T_ν is sufficiently small — we may approximate $f(x, y) \approx c_i^\nu$ for $(x, y) \in T_\nu$ by a constant. The integral (15.132) is then approximated by

$$b_i^\nu = \iint_{T_\nu} f\, \omega_i^\nu \, dx\, dy \approx c_i^\nu \iint_{T_\nu} \omega_i^\nu(x, y)\, dx\, dy = \tfrac{1}{3}\, c_i^\nu \,\text{area}\, T_\nu = \tfrac{1}{6}\, c_i^\nu \,|\, \Delta_\nu \,|. \tag{15.133}$$

The formula for the integral of the affine element $\omega_i^\nu(x, y)$ follows from solid geometry. Indeed, it equals the volume under its graph, a tetrahedron of height 1 and base T_ν, as illustrated in Figure 15.19.

How to choose the constant c_i^ν? In practice, the simplest choice is to let $c_i^\nu = f(x_i, y_i)$ be the value of the function at the i^{th} vertex. With this choice, the sum in (15.132) becomes

$$b_i \approx \sum_\nu \tfrac{1}{3}\, f(x_i, y_i) \,\text{area}\, T_\nu = \tfrac{1}{3}\, f(x_i, y_i) \,\text{area}\, P_i, \tag{15.134}$$

where P_i is the vertex polygon (15.118) corresponding to the node $\mathbf{x}_i$. In particular, for the square mesh with the uniform choice of triangles, as in Example 15.18,

$$\text{area}\, P_i = 3\, h^2 \qquad \text{for all } i, \text{ and so} \qquad b_i \approx f(x_i, y_i)\, h^2 \tag{15.135}$$

is well approximated by just h^2 times the value of the forcing function at the node. This is the underlying reason to choose the uniform triangulation for the square mesh; the alternating version would give unequal values for the b_i over adjacent nodes, and this would introduce unnecessary errors into the final approximation.

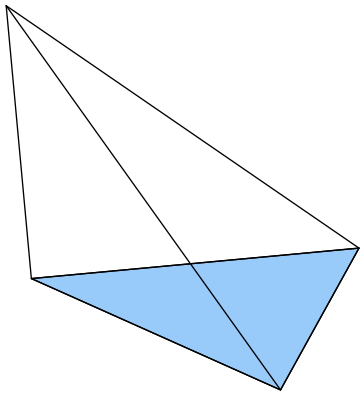

Figure 15.19. Finite Element Tetrahedron.

Example 15.21. For the coarsely triangulated oval plate, the reduced stiffness matrix is (15.131). The Poisson equation

$$-\Delta u = 4$$

models a constant external heat source of magnitude 4° over the entire plate. If we keep the edges of the plate fixed at 0°, then we need to solve the finite element equation $K\mathbf{c} = \mathbf{b}$, where K is the coefficient matrix (15.131), while

$$\mathbf{b} = \tfrac{4}{3}\left(2 + \tfrac{3\sqrt{3}}{4},\ 2,\ 2 + \tfrac{3\sqrt{3}}{4}\right)^T = (\,4.39872, 2.66667, 4.39872\,)^T.$$

The entries of $\mathbf{b}$ are, by (15.134), equal to $4 = f(x_i, y_i)$ times one third the area of the corresponding vertex polygon, which for node 2 is the square consisting of 4 right triangles, each of area $\frac{1}{2}$, whereas for nodes 1 and 3 it consists of 4 right triangles of area $\frac{1}{2}$ plus three equilateral triangles, each of area $\frac{\sqrt{3}}{4}$; see Figure 15.17.

The solution to the final linear system is easily found:

$$\mathbf{c} = (\,1.56724, 1.45028, 1.56724\,)^T.$$

Its entries are the values of the finite element approximation at the three interior nodes. The finite element solution is plotted in the first illustration in Figure 15.20. A more accurate solution, based on a square grid triangulation of size $h = .1$ is plotted in the second figure.

Inhomogeneous Boundary Conditions

So far, we have restricted our attention to problems with homogeneous Dirichlet boundary conditions. According to Theorem 15.15, the solution to the inhomogeneous Dirichlet problem

$$-\Delta u = f \quad \text{in} \quad \Omega, \qquad\qquad u = h \quad \text{on} \quad \partial\Omega,$$

is also obtained by minimizing the Dirichlet functional (15.103). However, now the minimization takes place over the affine subspace consisting of all functions that satisfy the

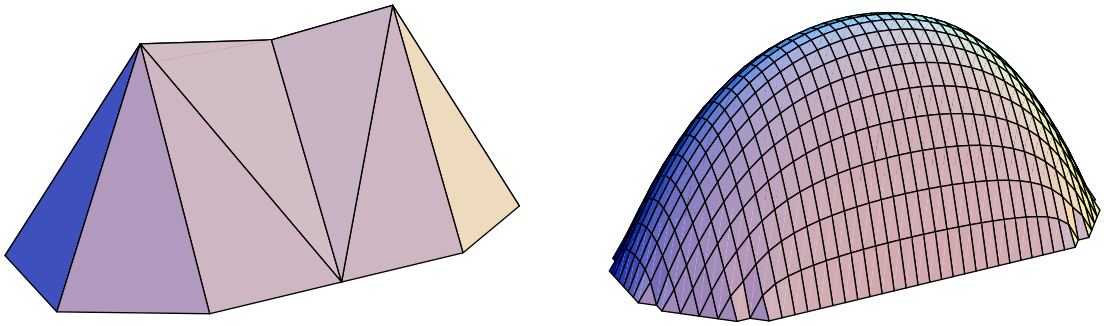

Figure 15.20. Finite Element Solutions to Poisson's Equation for an Oval Plate.

inhomogeneous boundary conditions. It is not difficult to fit this problem into the finite element scheme.

The elements corresponding to the interior nodes of our triangulation remain as before, but now we need to include additional elements to ensure that our approximation satisfies the boundary conditions. Note that if $\mathbf{x}_k$ is a boundary node, then the corresponding *boundary element* $\varphi_k(x,y)$ satisfies the interpolation condition (15.109), and so has the same piecewise affine form (15.117). The corresponding finite element approximation

$$w(x,y) = \sum_{i=1}^{m} c_i\, \varphi_i(x,y), \tag{15.136}$$

has the same form as before, (15.110), but now the sum is over all nodes, both interior and boundary. As before, the coefficients $c_i = w(x_i,y_i) \approx u(x_i,y_i)$ are the values of the finite element approximation at the nodes. Therefore, in order to satisfy the boundary conditions, we require

$$c_j = h(x_j,y_j) \qquad \text{whenever} \qquad \mathbf{x}_j = (x_j,y_j) \qquad \text{is a boundary node.} \tag{15.137}$$

Remark: If the boundary node $\mathbf{x}_j$ does not lie precisely on the boundary $\partial\Omega$, we need to approximate the value $h(x_j,y_j)$ appropriately, e.g., by using the value of $h(x,y)$ at the nearest boundary point $(x,y) \in \partial\Omega$.

The derivation of the finite element equations proceeds as before, but now there are additional terms arising from the nonzero boundary values. Leaving the intervening details to the reader, the final outcome can be written as follows. Let K^* denote the full $m \times m$ finite element matrix constructed as above. The reduced coefficient matrix K is obtained by retaining the rows and columns corresponding to only interior nodes, and so will have size $n \times n$, where n is the number of interior nodes. The *boundary coefficient matrix* $\widetilde{K}$ is the $n \times (m-n)$ matrix consisting of the entries of the interior rows that do not appear in K, i.e., those lying in the columns indexed by the boundary nodes. For instance, in the the coarse triangulation of the oval plate, the full finite element matrix is given in (15.130), and the upper 3×3 subblock is the reduced matrix (15.131). The remaining entries of the

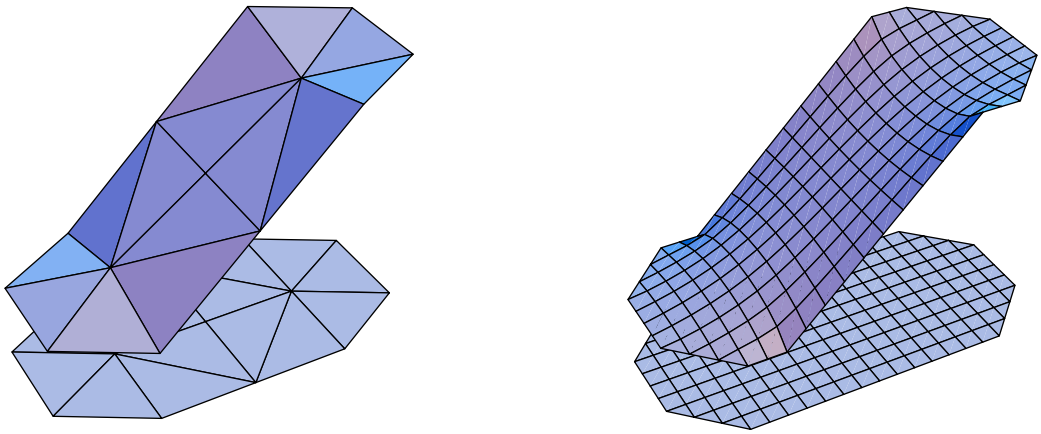

Figure 15.21. Solution to the Dirichlet Problem for the Oval Plate.

first three rows form the boundary coefficient matrix

$$\widetilde{K} = \begin{pmatrix} 0 & -.7887 & -.5774 & -.5774 & -.7887 & 0 & 0 & 0 & 0 & 0 \\ -1 & 0 & 0 & 0 & 0 & -1 & 0 & 0 & 0 & 0 \\ 0 & 0 & 0 & 0 & 0 & 0 & -.7887 & -.5774 & -.5774 & -.7887 \end{pmatrix}. \tag{15.138}$$

We similarly split the coefficients c_i of the finite element function (15.136) into two groups. We let $\mathbf{c} \in \mathbb{R}^n$ denote the as yet unknown coefficients c_i corresponding to the values of the approximation at the interior nodes $\mathbf{x}_i$, while $\mathbf{h} \in \mathbb{R}^{m-n}$ will be the vector of boundary values (15.137). The solution to the finite element approximation (15.136) is obtained by solving the associated linear system

$$K\,\mathbf{c} + \widetilde{K}\,\mathbf{h} = \mathbf{b}, \qquad \text{or} \qquad K\,\mathbf{c} = \mathbf{f} = \mathbf{b} - \widetilde{K}\,\mathbf{h}. \tag{15.139}$$

Example 15.22. For the oval plate discussed in Example 15.20, suppose the right hand semicircular edge is held at $10°$, the left hand semicircular edge at $-10°$, while the two straight edges have a linearly varying temperature distribution ranging from $-10°$ at the left to $10°$ at the right, as illustrated in Figure 15.21. Our task is to compute its equilibrium temperature, assuming no internal heat source. Thus, for the coarse triangulation we have the boundary nodes values $\mathbf{h} = (\,h_4, \dots, h_{13}\,)^T = (\,0, -1, -1, -1, -1, 0, 1, 1, 1, 1, 0\,)^T$. Using the previously computed formulae (15.131, 138) for the interior coefficient matrix K and boundary coefficient matrix $\widetilde{K}$, we approximate the solution to the Laplace equation by solving (15.139). We are assuming that there is no external forcing function, $f(x, y) \equiv 0$, and so the right hand side is $\mathbf{b} = \mathbf{0}$, and so we must solve $K\,\mathbf{c} = \mathbf{f} = -\widetilde{K}\,\mathbf{h} = (\,2.18564, 3.6, 7.64974\,)^T$. The finite element function corresponding to the solution $\mathbf{c} = (\,1.06795, 1.8, 2.53205\,)^T$ is plotted in the first illustration in Figure 15.21. Even on such a coarse mesh, the approximation is not too bad, as evidenced by the second illustration, which plots the finite element solution for a square mesh with spacing $h = .2$ between nodes.

